APPENDIX: Characterizing poliovirus transmission and evolution: Insights from modeling experiences with wild and vaccine-related polioviruses

Radboud J. Duintjer Tebbens,[1] Mark A. Pallansch,[2] Dominika A. Kalkowska,[1,3] Steven G.F. Wassilak,[4] Stephen L. Cochi,[4] Kimberly M. Thompson[1,5]

1. Kid Risk, Inc., 10524 Moss Park Rd., Ste. 204-364, Orlando, FL, USA

2. Division of Viral Diseases, National Center for Immunization and Respiratory Diseases, Centers for Disease Control and Prevention, Atlanta, GA, USA

3. Delft Institute of Applied Mathematics, Delft University of Technology, Delft, Netherlands

4. Global Immunization Division, Center for Global Health, Centers for Disease Control and Prevention, Atlanta, GA, USA

5. University of Central Florida, College of Medicine, Orlando, FL, USA

This appendix provides the equations (A1), details about multi-stage processes used (A2), calculation of effective mortality rates in the model (A3), documentation of model inputs that change over time (A4), and supplemental results (A5). We use the same acronyms and we refer to Tables and Figures as in the main paper, but we provide additional Tables and Figures in the appendix preceded by an "A" to distinguish them from those from main text. The appendix uses its own list of references provided at the end and different from the main paper.

A1. Equations

We define the following indices and symbols for the full generic model equations. The symbols correspond to those used in the main paper, although in some instances the indices for a symbol differ because the main paper omitted non-essential indices for the main methods description (e.g., the main methods description shows a single index for the pair (immunity state, waning stage) and shows the excretion mode as a superscript (e.g., $\pi_{i,w,o}$ is the same as π_i^{fec} in the main paper)).

Indices:

a = situation-specific age group (a = 0,…, na-1, where na depends on the situation and age group 0 is always from 0-2 months, inclusive; note that maternally immunes only exist in age group 0)

a_m = mixing age group (a_m=0,…,na_m-1, where typically na_m=3 with a_m=0 (0-4 years), 1 (5-14 years), 2 (15 or more years))

$A(a)$ = mixing matrix age group that situation-specific age group a belongs to (i.e., $A(a)=a_m$ if situation-specific age group a belongs to mixing age group a_m)

$c(a_m)$ = cut-off for mixing age group a_m = first situation-specific age group included in mixing age group a_m, where we define $c(na_m)=na_m$

e = excretion and transmission mode (e = 0 (fecal) or 1 (oropharyngeal))

fa = first situation-specific age group for which we assume immunes can give birth to children with maternal immunity

i = immunity state (i = 0 (fully susceptible), 1 (maternally immune), 2 (1 successful IPV), 3 (2 successful IPV, 4 (≥ 3 successful IPV), 5 (1 LPV infection), 6 (≥ 2 LPV infections) ,7 (IPV and LPV))

j = virus strain (j = 0 (OPV), 1,…, h-2 (OPV-related), h-1 (FRPV), h (WPV), where h=20)

k = infection stage (k = 0 (first latent stage), r-1(last latent stage), r (first infectious stage), …, r+s-1 (last infectious stage), where r=2 and s=4)

la = last situation-specific age group for which we assume immunes can give birth to children with maternal immunity

w = waning stage (w = 0 (recent),…, nw -1, where nw=5; note that fully susceptibles and maternally immunes only exists in waning stage 0)

Symbols for state variables:

$IPVE_{a,i,w}$ = successfully IPV-vaccinated individuals from immunity state i, age group a, and waning stage w that have not yet acquired the properties of the next IPV state (i.e., IPV-exposed individuals)

$LI_{a,i,w,j,k,e}$ = individuals from immunity state i, age group a, and waning stage w infected with live virus strain j and residing in infection stage k of excretion mode e (i.e., live-virus-infected individuals)

$PI_{a,i,w}$ = partially infectible individuals in immunity state i, age group a, and waning stage w

Other symbols:

α = seasonal amplitude of R_0 (for any strain) (i.e., difference from the average R_0 at peak or through, relative to the average R_0)

b = birth rate [1/(people × days)]

$\gamma_{i,w,e}$ = total duration of infectious period (in all infectious stages) for immunity state i, waning stage w, and excretion mode e [days]

$EPI_{a,j}$ = effective proportion infectious to situation-specific age group a with virus strain j

$EPIM_{am,j,e}$ = effective proportion infectious to mixing age group m_a with virus strain j with respect to excretion mode e

EPI^* = effective proportion infectious below which we assume 0 force-of-infection (i.e., the transmission threshold)

evc_a^{IPV} (evc_a^{OPV}) = effective vaccination coverage with IPV (OPV) = fraction of the population receiving an effective IPV (OPV) dose upon entering situation-specific age group a (i.e., a dose that takes if given to a fully susceptible individual)

evr_a^{IPV} (evr_a^{OPV}) = effective IPV (OPV) vaccination rate = fraction of the population in situation-specific age group a receiving an effective IPV (OPV) dose per day (i.e., a dose that takes if given to a fully susceptible) [1/day]

ε = average time to reach last reversion stage [days]

φ = IPV immunity delay [days]

θ_k = relative infectiousness weight of infection stage k

$\kappa(a_m)$ = proportion of potentially infectious contacts of individuals in mixing age group a_m reserved for individuals within the same mixing age group

$\lambda_{a,j}$ = force-of-infection to situation-specific age group a due to virus strain j [1/days]

mf = fraction of newborns born with maternal immunity

μ_a = fraction of people in situation-specific age group a that die (or emigrate) per day [1/days]

μ^{ave} = fraction of all people that die (or emigrate) per day [1/days]

$M(a_m,b_m)$ = mixing matrix containing normalized mixing coefficients for potentially infectious contacts of individuals in mixing age group a_m with individuals in mixing age group b_m

$MNI_{a,i}$ = inflow for partially infectibles in situation-specific age group a and immunity state i due to individuals moving to the next IPV state after leaving the IPVE state [people/days]

$MNL_{a,i}$ = inflow for partially infectibles in situation-specific age group a and immunity state i due to individuals moving to the next LPV state after recovering from infection [people/days]

N = total population size [people]

N_a = total population size in age group a [people]

NM_{a_m} = total population size in mixing age group a_m [people]

PIR_j = paralysis-to-infection ratio (PIR) for fully susceptible individuals infected with virus strain j based on functional form for PIR by reversion stage (see methods)

$RPIR^{MI}$ = relative PIR for maternally immunes compared to fully susceptibles

$RPIR_a^{age}$ = relative PIR for fully susceptible individuals in situation-specific age group a compared to the first age group

$\pi_{i,w,e}$ = relative infectiousness for immunity state i, waning stage w, and excretion mode e

$R0_j$ = R_0 for virus strain j (as a function of time)

$R0^{ave}_j$ = average R_0 for virus strain j based on functional form for relative R_0 by reversion stage (see methods)

p_e = proportion of transmissions via excretion mode e (p_0 =1-p^{oro} and $p_1 = p^{oro}$)

pd = seasonal peak day for R_0 [day number in each year]

ρ = average time to reach the last waning stage [days]

$\sigma_{i,w}$ = relative susceptibility for immunity state i in waning stage w

τ = relative R_0 of OPV vs. homotypic FRPV and WPV

w_a = width of age group a (with $w_0 = \rho_{MI} = 0.25\times365$ days (Table 1)) [days]

$\xi_{i,w,e}$ = duration of latent period for immunity state i, waning stage w, and excretion mode e [days]

z_p = shape parameter for the relationship between PIR and reversion stage

z_r = shape parameter for the relationship between R_0 and reversion stage

z_w = shape parameter of the waning functions

The equation structure does not vary by serotype and we omit serotype-dependence for ease of presentation, although we use serotype-specific model inputs as appropriate (see Tables I-XII). To shorten the equations, we use the indicator function $1_{\{c1,c2,\ldots\}}$ that equals 1 if all conditions c1,c2,.. are true and 0 otherwise. The first 3 equations below represent the full set of differential equations represented in Figure 1b. The last 2 equations reflect the flows between immunity states shown in Figure 1a. The intermediate equations provide the equations of intermediate quantities that we introduce to simplify the notation for the differential equations. We solve the differential equations using Euler integration with a step size of 0.125 days. This approximates $1/10^{th}$ of the smallest time constant in the model (i.e., the two latent stages of ~ 1.5 days each).

$$\begin{aligned}\frac{dPI_{a,i,w}(t)}{dt} = {} & b(t)N(t)\Big(\big(1-mf(t)\big)\big(1-evc_0^{IPV}(t)-evc_0^{OPV}(t)\big)1_{\{i=0\}} \\ & + mf(t)\Big(1-evc_0^{IPV}(t)-\sigma_{1,0}evc_0^{OPV}(t)\Big)1_{\{i=1\}}\Big)1_{\{a=0\}} \\ & + \Big(1-evc_{a-1}^{IPV}(t)-\sigma_{i,w}evc_{a-1}^{OPV}(t)\Big)\big(PI_{a-1,i,w}(t)+PI_{0,1,0}(t)1_{\{a=1,i=0\}}\big)\frac{1_{\{a>0\}}}{w_{a-1}} \\ & + \Big(MNL_{a,i}(t)+MNI_{a,i}(t)\Big)1_{\{w=0\}} + PI_{a,i,w-1}(t)\frac{nw-1}{\rho}1_{\{w>0,i>1\}} \\ & - \Bigg\{\mu_a(t)+\frac{1_{\{a<na-1\}}}{w_a}+\sum_{j=0}^{h}\sigma_{i,w}\lambda_{a,j}(t)+\sigma_{i,w}evr_a^{OPV}(t)+evr_a^{IPV}(t) \\ & \qquad + \frac{nw-1}{\rho}1_{\{w<nw-1,i>1\}}\Bigg\}PI_{a,i,w}(t)\end{aligned}$$

$$\begin{aligned}\frac{dIPVE_{a,i,w}(t)}{dt} = {} & b(t)N(t)evc_0^{IPV}(t)\Big(\big(1-mf(t)\big)1_{\{i=0\}}+mf(t)1_{\{i=1\}}\Big)1_{\{a=0\}} \\ & + \big(IPVE_{a-1,i,w}(t)+IPVE_{0,1,0}(t)1_{\{a=1,i=0\}}+evc_{a-1}^{IPV}(t)PI_{a-1,i,w}(t) \\ & + evc_{a-1}^{IPV}(t)PI_{0,1,0}(t)1_{\{a=1,i=0\}}\big)\frac{1_{\{a>0\}}}{w_{a-1}}+IPVE_{a,i,w-1}(t)\frac{nw-1}{\rho}1_{\{w>0,i>1\}} \\ & + evr_a^{IPV}(t)PI_{a,i,w}(t) \\ & - \Bigg\{\mu_a(t)+\frac{1_{\{a<na-1\}}}{w_a}+\sum_{j=0}^{h}\sigma_{i,w}\lambda_{a,j}(t)+\sigma_{i,w}evr_a^{OPV}(t) \\ & + \frac{nw-1}{\rho}1_{\{w<nw-1,i>1\}}+1/\varphi\Bigg\}IPVE_{a,i,w}(t)\end{aligned}$$

$$\frac{dLI_{a,i,w,j,k,e}(t)}{dt}$$
$$= b(t)N(t)evc_0^{OPV}(t)\Big(\big(1-mf(t)\big)1_{\{i=0\}}+\sigma_{1,0}mf(t)1_{\{i=1\}}\Big)\,1_{\{a=0,j=0,k=0\}}$$
$$+\big(LI_{a-1,i,w,j,k,e}(t)+LI_{0,1,0,j,k,e}(t)1_{\{a=1,i=0\}}$$
$$+\sigma_{i,w}evc_{a-1}^{OPV}(t)PI_{a-1,i,w}(t)1_{\{j=0,k=0\}}$$
$$+evc_0^{OPV}(t)PI_{0,1,0}(t)1_{\{a=1,i=0,j=0,k=0\}}\big)\frac{1_{\{a>0\}}}{w_{a-1}}$$
$$+\big(evr_a^{OPV}(t)1_{\{j=0\}}+\lambda_{a,j}(t)\big)\sigma_{i,w}PI_{a,i,w}(t)1_{\{k=0\}}+\frac{LI_{a,i,w,j,k-1,e}(t)r}{\xi_{i,w,e}}1_{\{0<k\le r\}}$$
$$+\frac{LI_{a,i,w,j,k-1,e}(t)s}{\gamma_{i,w,e}}1_{\{k>r\}}+\frac{LI_{a,i,w,j-1,k,e}(t)(h-1)}{\varepsilon}1_{\{0<j<h\}}$$
$$-\left\{\mu_a(t)+\frac{1_{\{a<na-1\}}}{w_a}+\frac{r}{\xi_{i,w,e}}1_{\{k<r\}}+\frac{s}{\gamma_{i,w,e}}1_{\{k\ge r\}}\right.$$
$$\left.+\frac{h-1}{\varepsilon}1_{\{j<h-1\}}\right\}LI_{a,i,w,j,k,e}(t)$$

$$N_a(t)=\left(PI_{0,1,0}(t)+IPVE_{0,1,0}(t)+\sum_{j=0}^{h}\sum_{k=0}^{r+s-1}LI_{0,1,0,j,k,0}(t)\right)1_{\{a=0\}}+PI_{a,0,0}(t)$$
$$+IPVE_{a,0,0}(t)+\sum_{j=0}^{h}\sum_{k=0}^{r+s-1}LI_{a,0,0,j,k,0}(t)$$
$$+\sum_{i=2}^{ni-1}\sum_{w=0}^{nw-1}\left(PI_{a,i,w}(t)+IPVE_{a,i,w}(t)+\sum_{j=0}^{h}\sum_{k=0}^{r+s-1}LI_{a,i,w,j,k,0}(t)\right)$$

$$N(t)=\sum_{a=0}^{na-1}N_a(t)$$

$$NM_{a_m}(t)=\sum_{b=c(a_m)}^{c(a_m+1)}N_b(t)$$

$$mf(t)=\frac{\sum_{a\ge fa}^{la}\sum_{i=3}^{ni-1}\sum_{w=0}^{nw-1}PI_{a,i,w}(t)}{+\sum_{a\gg fa}^{la}N_a(t)}$$

$$EPIM_{a_m,j,e}(t) = \sum_{k=r}^{r+s-1} \sum_{b=c(a_m)}^{c(a_m+1)} \Bigg(LI_{0,1,w,j,k,e}(t)\pi_{1,0,e} M(a_m,0)(t) 1_{\{b=0\}} + \Bigg(LI_{a,0,w,j,k,e}(t)\pi_{0,0,e} + + \sum_{i=2}^{7} \sum_{w=0}^{nw-1} LI_{a,i,w,j,k,e}(t)\pi_{i,w,e} \Bigg) M\big(a_m, A(b)\big)(t) \Bigg) \frac{\theta_k}{NM_{a_m}(t)}$$

$$EPI_{a,j}(t) = \sum_{e=0}^{1} EPIM_{A(a),j,e}(t) p_e$$

$$\lambda_{a,j}(t) = 1_{EPI_{a,j}(t) \geq EPI^*} \sum_{e=0}^{1} EPIM_{A(a),j,e}(t) p_e (1/\gamma_{0,0,e} + \mu^{ave}) R0_j(t)$$

$$\mu^{ave}(t) = \sum_{a=0}^{na-1} \mu_a(t) N_a(t)/N(t)$$

$$R0_j(t) = R0_j^{ave} \left(1 + R0^{ampl} \times \sin\left(\left(t - \frac{pd}{365}\right) 2\pi + \frac{\pi}{2}\right)\right)$$

$$R0_j^{ave} = R0_{h-1}^{ave} - (R0_{h-1}^{ave} - R0_0^{ave}) \times ((h-1-\mathrm{j})/(h-1))^{z_r}, \quad j = 1,\ldots,h\text{-}1$$

$$R0_{h-1}^{ave} = R0_h^{ave}$$

$$R0_0^{ave} = \tau R0_h^{ave}$$

$$M(a_m, b_m)(t) = \kappa(a_m) 1_{\{a_m = b_m\}} + \frac{\big(1-\kappa(a_m)\big)\big(1-\kappa(b_m)\big) NM_{b_m}(t)}{\sum_{b=0}^{na_m-1} NM_b(t)\big(1-\kappa(b)\big)}$$

$$\sigma_{i,w} = \sigma_{i,nw-1} - (\sigma_{i,nw-1} - \sigma_{i,0}) \times ((w-1-\mathrm{j})/(w\ -1))^{z_w}$$

$$\gamma_{i,w,e} = \gamma_{i,nw-1,e} - (\gamma_{i,nw-1,e} - \gamma_{i,0,e}) \times ((w-1-\mathrm{j})/(w\ -1))^{z_w}$$

$$\pi_{i,w,e} = \pi_{i,nw-1,e} - (\pi_{i,nw-1,e} - \pi_{i,0,e}) \times ((w-1-\mathrm{j})/(w\ -1))^{z_w}$$

$$\xi_{i,w,e} = \xi_{i,0,e}$$

$$\begin{aligned} MNI_{a,i}(t) = {} & \left(IPVE_{a,0,0}(t) + IPVE_{0,1,0}(t)1_{\{a=0\}}\right)1_{\{i=2\}}/\varphi \\ & + \sum_{w=0}^{nw-1} \left(IPVE_{a,2,w}(t)1_{\{i=3\}} + \left(IPVE_{a,3,w}(t) + IPVE_{a,4,w}(t)\right)1_{\{i=4\}}\right. \\ & \left. + \left(IPVE_{a,5,w}(t) + IPVE_{a,6,w}(t) + IPVE_{a,7,w}(t)\right)1_{\{i=7\}}\right)/\varphi \end{aligned}$$

$$\begin{aligned} MNL_{a,i}(t) = {} & \sum_{j=0}^{h} \left(LI_{a,0,0,j,r+s-1,0}(t)/\gamma_{0,0,0} + LI_{0,1,0,j,r+s-1,0}(t)1_{\{a=0\}}/\gamma_{1,0,0}\right)s1_{\{i=5\}} \\ & + \sum_{w=0}^{nw-1} \left(\left(LI_{a,5,w,j,r+s-1,0}(t)/\gamma_{5,w,0} + LI_{a,6,w,j,r+s-1,0}(t)/\gamma_{6,w,0}\right)1_{\{i=6\}}\right. \\ & + \left(LI_{a,2,w,j,r+s-1,0}(t)/\gamma_{2,w,0} + LI_{a,3,w,j,r+s-1,0}(t)/\gamma_{3,w,0}\right. \\ & \left.\left. + LI_{a,4,w,j,r+s-1,0}(t)/\gamma_{4,w,0} + LI_{a,7,w,j,r+s-1,0}(t)/\gamma_{7,w,0}\right)1_{\{i=7\}}\right)s \end{aligned}$$

The equations derive from and depend on several important assumptions. First, we assume that the IPV take rates already account for any effect of maternal antibodies on the per-dose take rate, which evc^{IPV} incorporates. However, for maternally immune infants who receive OPV at birth we multiply the effective vaccination coverage by their relative susceptibility, and thus the evc^{OPV} calculation can use the same per-dose take rate regardless of timing of the first dose. This structural difference between how we handle IPV and OPV given to maternally immune infants preserves consistency in our assumption that IPV boosts already primed or immune individuals in other immunity states at the same rate as fully susceptible, while remaining more convenient by allowing us to use the same average per-dose OPV take rates in the context of birth doses or SIA doses reaching infants before their maternal immunity wanes. Second, we assume that maternally immune infants that receive a routine dose at 3 months flow into the IPV-exposed state (if given IPV) or LPV-infected state (if given OPV) for previously fully susceptible individuals (i.e., see equations for $\mathrm{IPVE}_{1,0,0}$ and $\mathrm{LI}_{1,0,0,0,0,e}$). We assume no effect of residual maternal immunity on take at 3 months of age (i.e., we do not multiply by relative susceptibility). Third, as mentioned in the main paper, oropharyngeal infection stages exist as a co-flow and

therefore individuals do not recover into the next LPV state (equation for $MNL_{a,i}$) or get counted towards the population size (equation for N_a) (i.e., oropharyngeal infection occurs coincident to fecal-oral infection). Fourth, the expression for the normalized preferential mixing matrix $M(a_m,b_m)$ corresponds to that proposed by Jacquez et al. (1988).[1] Fifth, to simplify the calculations, the formula for the force-of-infection takes the average net duration of the infectious period taking into account mortality as 1/(recovery rate + death rate) rather than the more cumbersome expression of a multi-stage infection process.[2] Given that the mortality rate remains much lower than the recovery rate in any or all stages, the approximation of the death rate based on a single-stage infection process leads to negligible error.

In situations with two interacting subpopulations (i.e., The Netherlands, northern Nigeria, and western Uttar Pradesh (WUP)), we follow our prior approach to characterize mixing between subpopulations.[3] Specifically, if the under-vaccinated subpopulation represents one of m hypothetical subpopulations, and using superscript 0 and 1 to denote the under-vaccinated and the general subpopulations, respectively, the force-of-infection in the under-vaccinated subpopulation equals:

$$\lambda^0_{a,j}(t) = 1_{EPI_{a,j}(t)\geq EPI^*} \sum_{e=0}^{1} \left(EPIM^0_{A(a),j,e}(t)p_{within} + EPIM^1_{A(a),j,e}(t)(1-p_{within})\right)p_e(1/\gamma_{0,0,e} + \mu^{ave})R0_j(t)$$

The force-of-infection for the general population equals:

$$\lambda^1_{a,j}(t) = 1_{EPI_{a,j}(t)\geq EPI^*} \sum_{e=0}^{1} \left(\frac{EPIM^0_{A(a),j,e}(t)(1-p_{within})}{m-1} + EPIM^1_{A(a),j,e}(t)\left(\frac{(1-p_{within})(m-2)}{m-1} + p_{within}\right)\right)p_e(1/\gamma_{0,0,e} + \mu^{ave})R0_j(t)$$

We compute the incidence of paralytic cases ($PPa_{,j}$) in situation-specific age group a due to virus strain j from the force-of-infection as follows:

$$PP_{a,j}(t) = \lambda_{a,j}(t-\delta)PIR_j\left(\sigma_{1,0}PI_{0,1,0}(t-\delta)RPIR^{MI}1_{\{a=0\}} + PI_{a,0,0}(t-\delta)RPIR_a^{age}\right)$$

$$PIR_j = PIR_{h-1} - (PIR_{h-1} - PIR_0) \times ((h-1-j)/(h-1))^{z_r}, \quad j = 1,\ldots,h\text{-}1$$

$$PIR_{h-1} = PIR_h$$

We compute non-recipient VAPP incidence as the sum of the incidence for virus strains 0 to h-2 (i.e., all VAPP due to contact infections except those from FRPVs) and VDPV incidence as the incidence from virus strain h-1 (i.e., only FRPVs). We compute recipient VAPP incidence from the sum of all OPV infections in fully susceptibles and maternally immunes due to evc_a^{OPV} and evr_a^{OPV} and using PIR_0. For vaccine given at time of aging from maternally immune to fully susceptible (i.e., at 3 months of age), we assume the relative PIR for maternally immunes still applies.

A2. Details about multi-stage processes for infection, waning, and reversion

This section provides details about processes modeled over multiple stages, including infectiousness, waning, and reversion. To generate the figures in this section, we introduce a pulse of individuals into the first stage of a process and follow how the average properties for this population change as a result of progression through the multiple stages and their assumed properties. We include these figures to show the implied distributions in the model as a result of our assumptions by discrete stages in the process, although we do not include the effect of mortality or any other flows on the flows between stages here, which in the actual model depend on the specific population modeled and influence the distributions as well. The figures for infection in this section reflect the model inputs for type 1, with similar values for types 2 and 3 that lead to slight differences in the results that did not warrant inclusion as additional figures. For the waning curves, we also show the values for types 1 which remain almost identical to type 2 (i.e., only the starting points differ slightly (Table I)). For type 3, the same patterns occur (not shown), but the increase occurs more rapidly due to the assumed shorter time to reach the last waning stage for type 3 compared to types 1 and 2 (Table I). Given relatively large differences in OPV reversion by serotype, we include separate figures for all 3 types to show the differences.

Figure A1 shows the distributions for the duration of fecal and oropharyngeal infectiousness implied by the 2 latent and 4 infectious stages in the model compared with the mean assessment obtained from the experts.[4] Figure A2 shows the average level of infectiousness for a population infected at time 0 assuming either constant infectiousness or the empirically fitted relative infectiousness by infectious stage according to the ratio 3:10:3:1 and compares these with the expert assessments based on the proportion excreting and relative infectiousness for the average titers excreted over time.[4] In these figures, we rescaled the curves so that the areas under the curves remain fixed to better compare the 3 curves within each plot. The unscaled infectious curves differ much more between immunity states due to the relative infectiousness compared to fully susceptible individuals ($\pi_{i,w,e}$) and differences in duration of infectiousness ($\gamma_{i,w,e}$). Figure A2 motivated the assumptions related to different levels of infectiousness by infectious stage to better match the expert assessments about infectiousness over time.

Figure A1: Distribution of the duration of fecal and oropharyngeal infectiousness in the model (solid blue line) and according to the means of expert assessments (black dashed line),[4] by immunity state

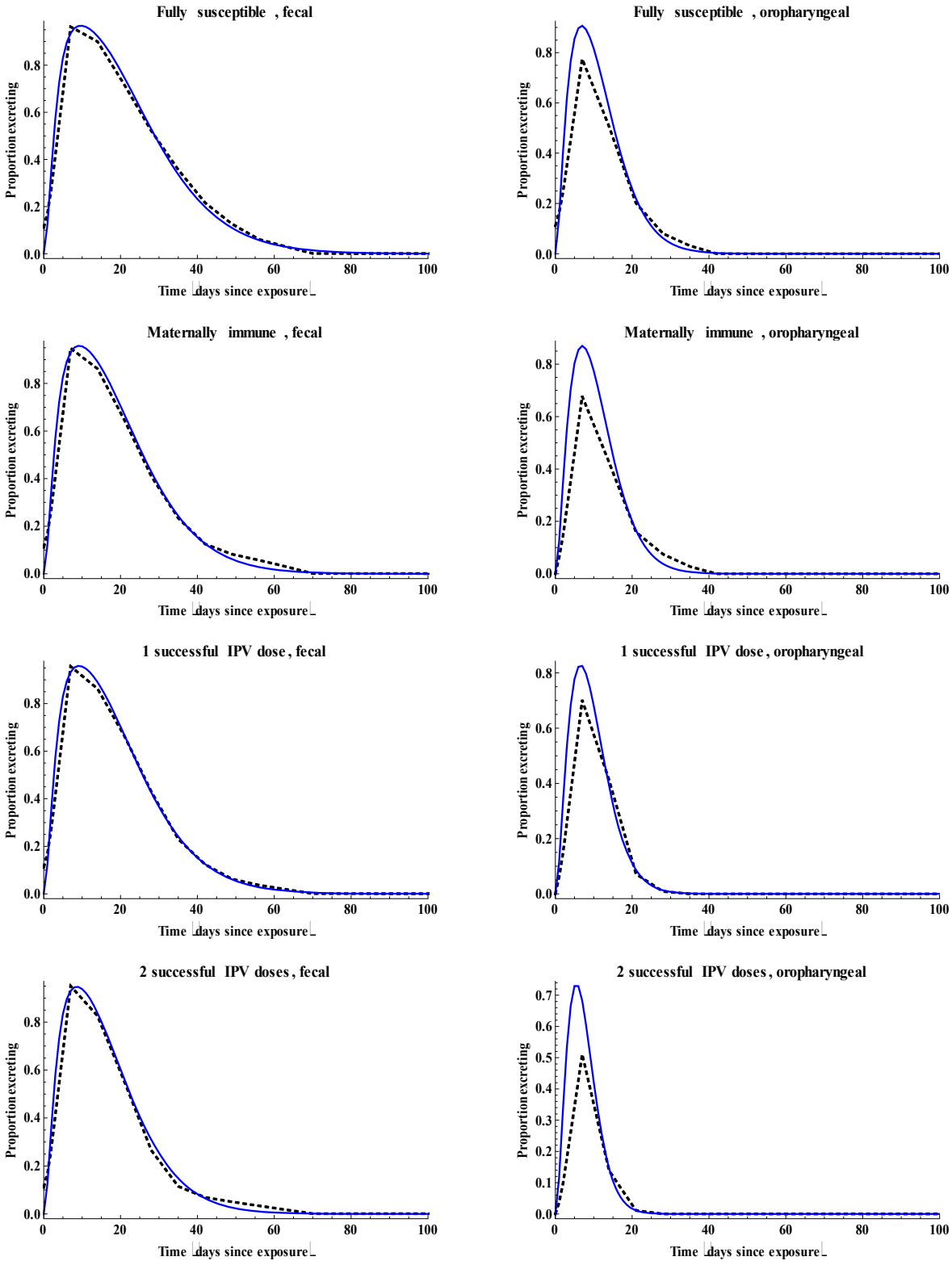

Figure A1 (cont'd): Distribution of the duration of fecal and oropharyngeal infectiousness in the model (solid blue line) and according to the means of expert assessments (dashed black line),[4] by immunity state

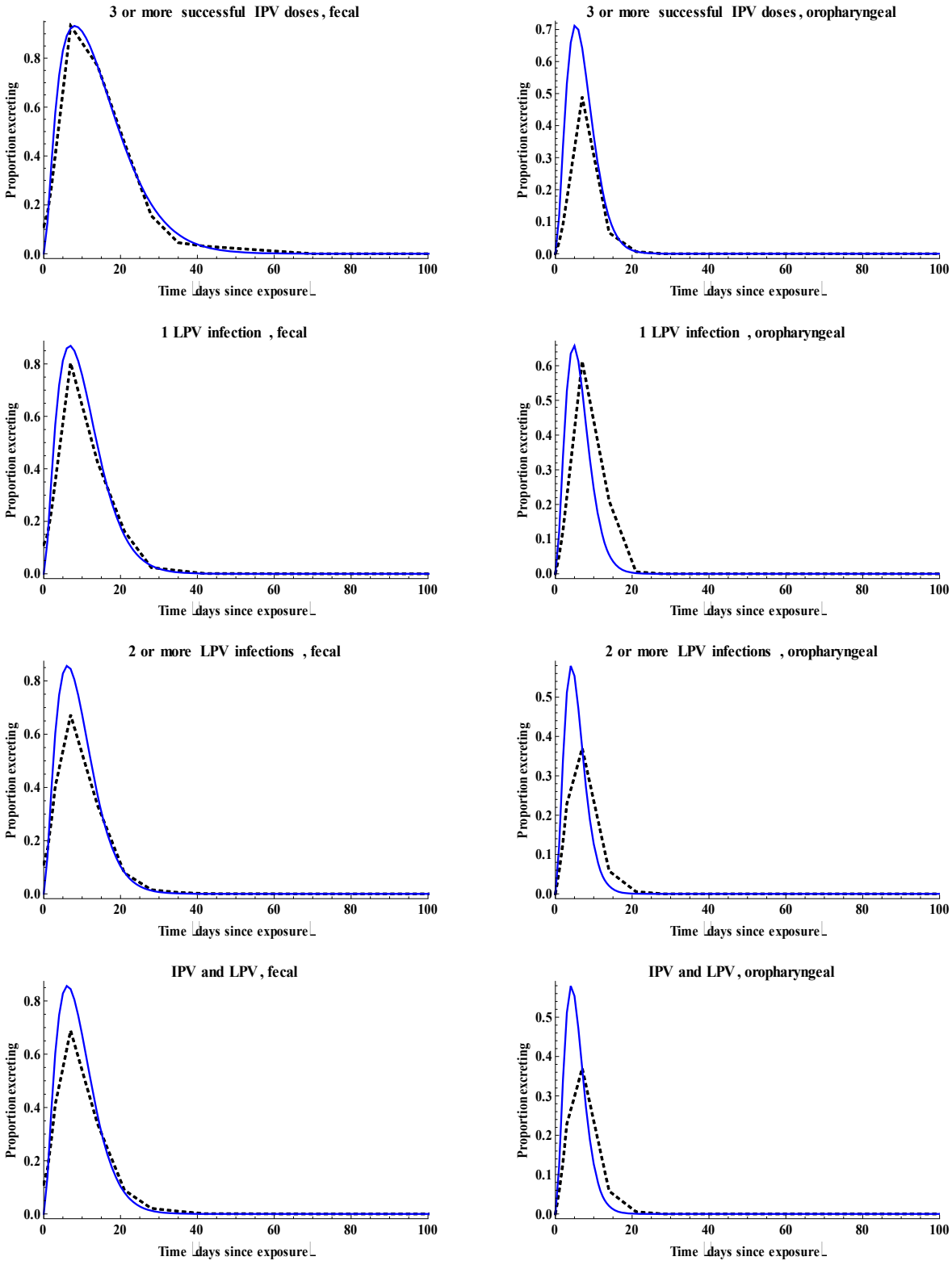

Figure A2: Average relative infectiousness for a population infected at time 0 according to expert assessments (dashed black line),[4] the model with constant infectiousness (dash-dotted red line), and the model with variable infectiousness by stage (solid blue line), by immunity state.

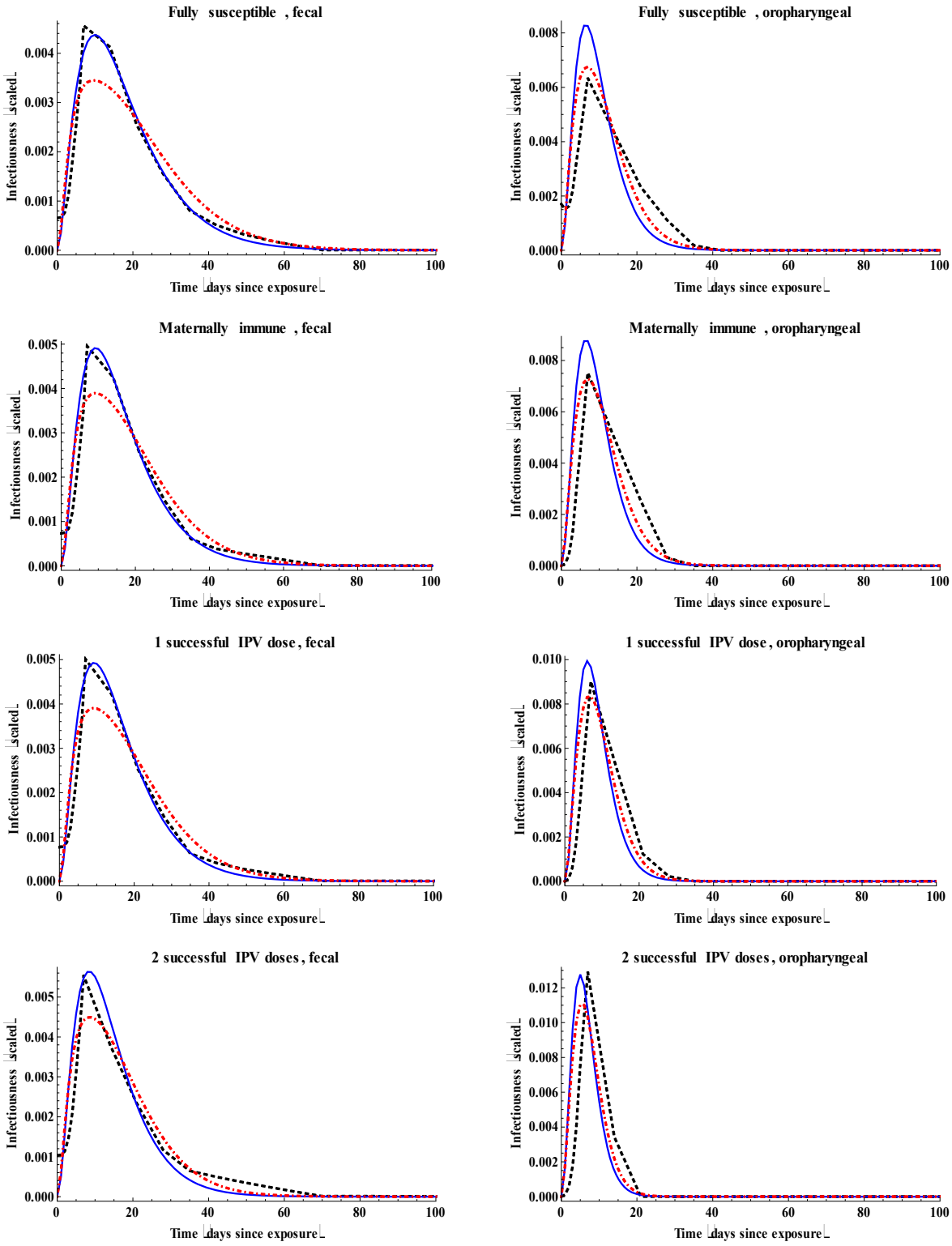

Figure A2 (cont'd): Average relative infectiousness for a population infected at time 0 according to expert assessments (dashed black line),[4] the model with constant infectiousness (dash-dotted red line), and the model with variable infectiousness by stage (solid blue line), by immunity state.

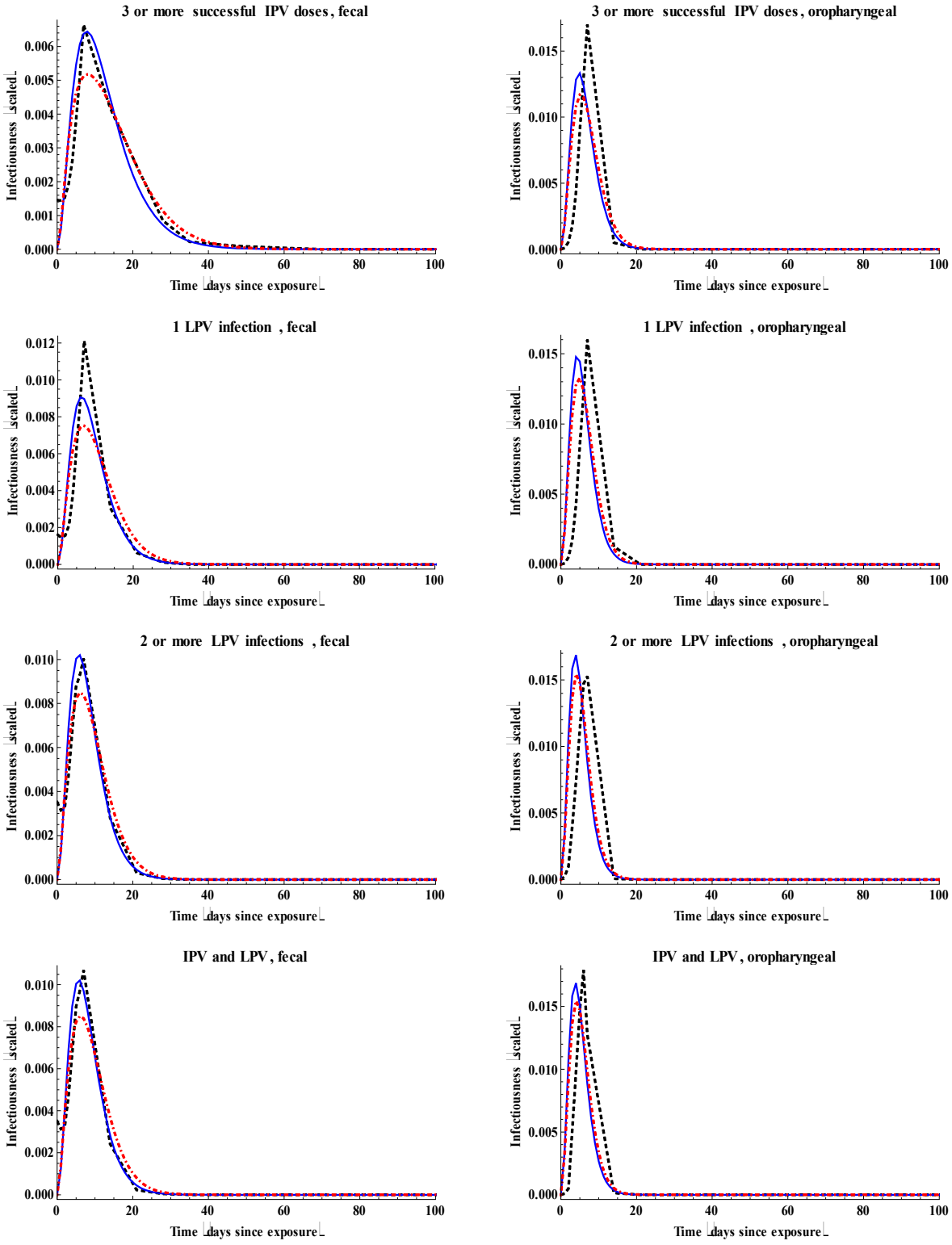

Figure A3 shows the average relative contribution to transmission compared to fully susceptible individuals, defined as the product of relative susceptibility, relative duration infectiousness, and relative infectiousness, for each active immunity state as a function of the time after entering an immunity state (in the absence of further infections or vaccinations), based on the model inputs for waning in Table I. The experts expressed significant uncertainty about waning, which led us to consider a very wide range for the input values.[4] Figure A3 shows that in the model we assumed less waning than the mean of the uncertain expert assessments as a result of fitting the model. Figure A3 includes both the inputs at each stage and the effective average values that resulted from the multi-stage waning process that we modeled, which produces slightly slower waning due to the steady-state error,[5] but converges to the model input values.

Figure A3: Waning curves for active immunity states, for type 1.

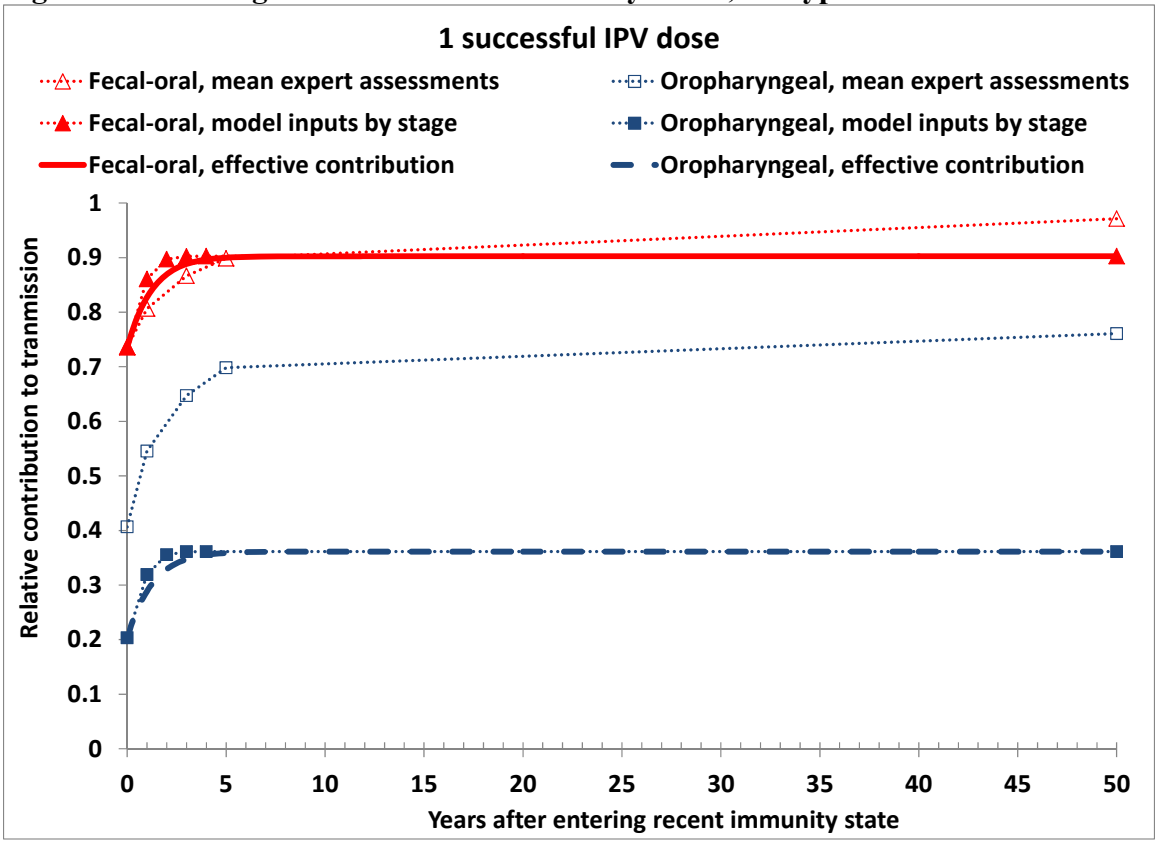

Figure A3 (cont'd): Waning curves for active immunity states for type 1.

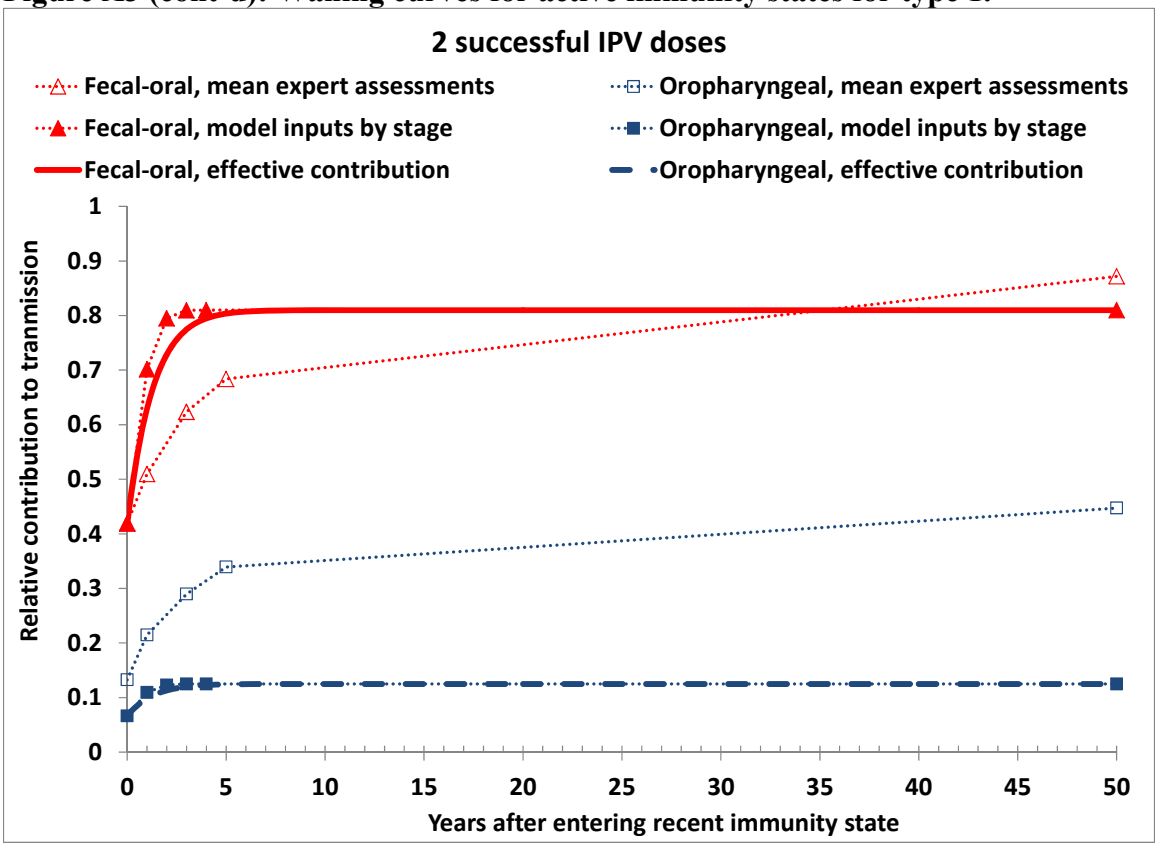

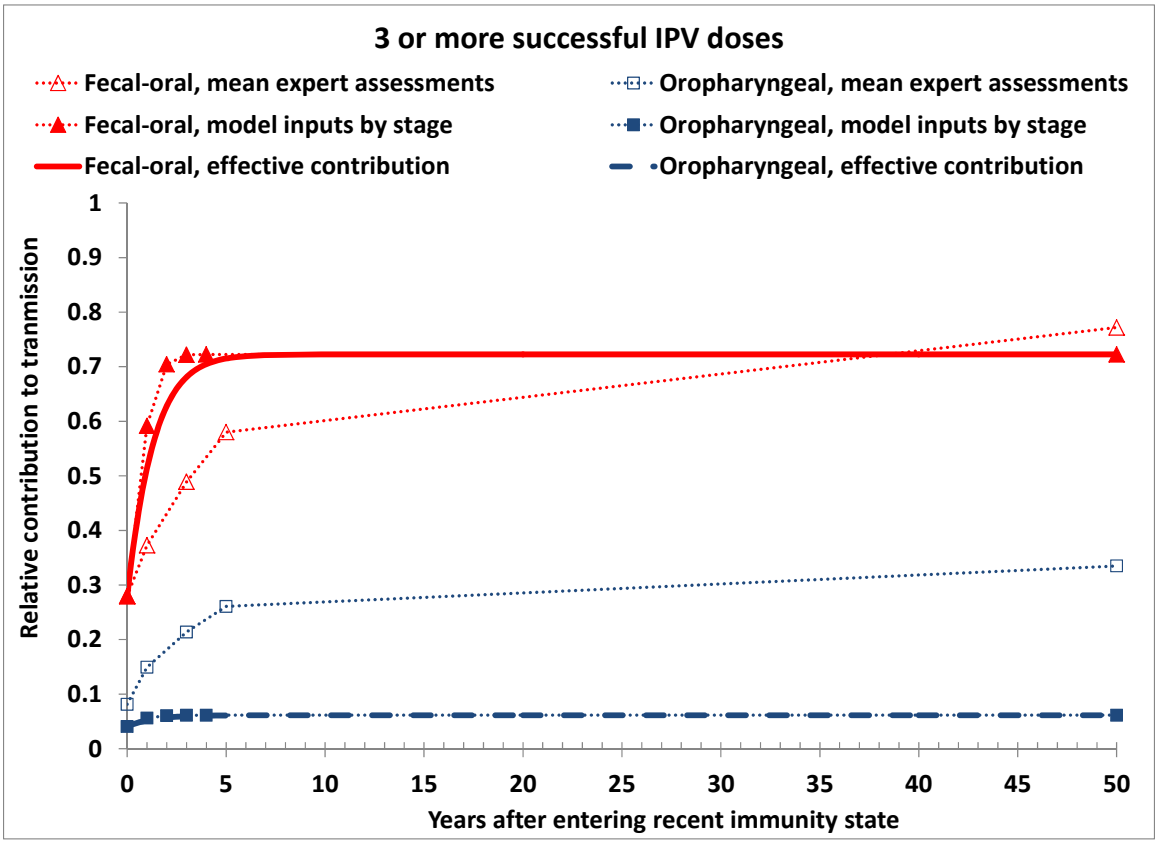

Figure A3 (cont'd): Waning curves for active immunity states for type 1.

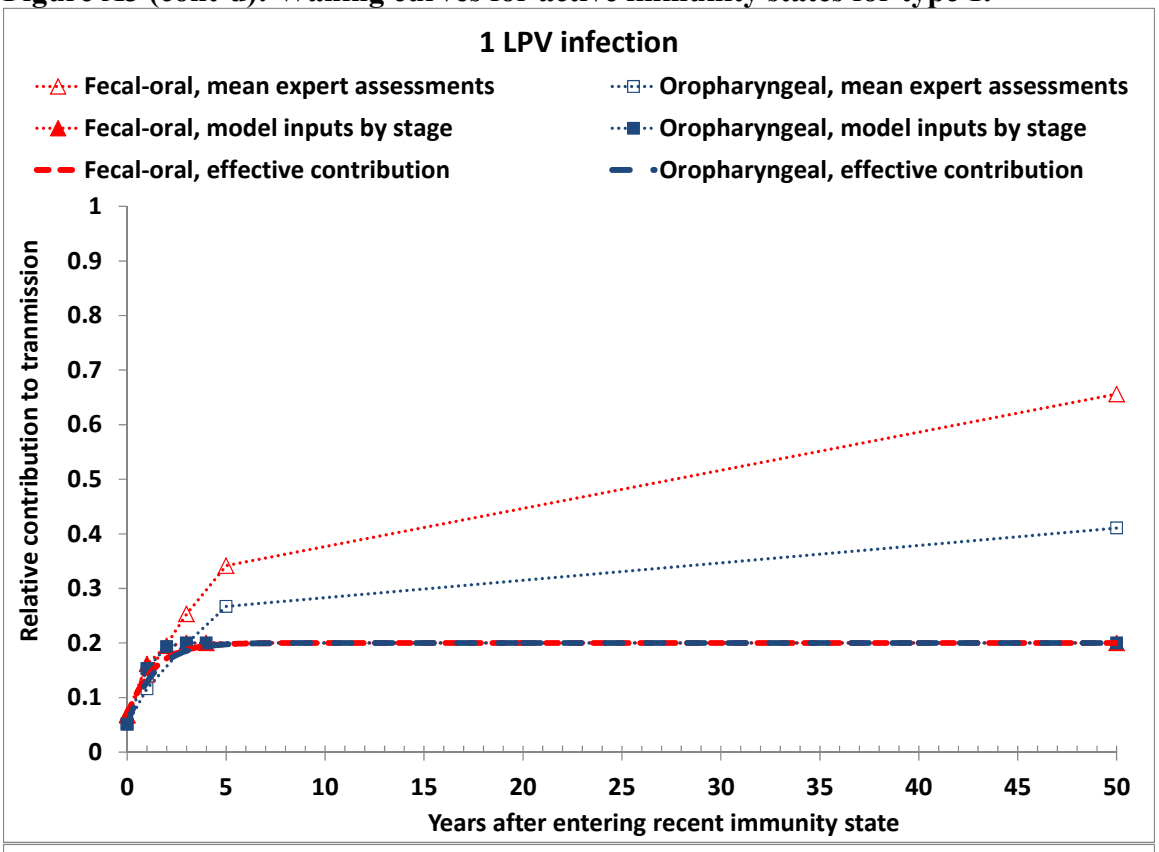

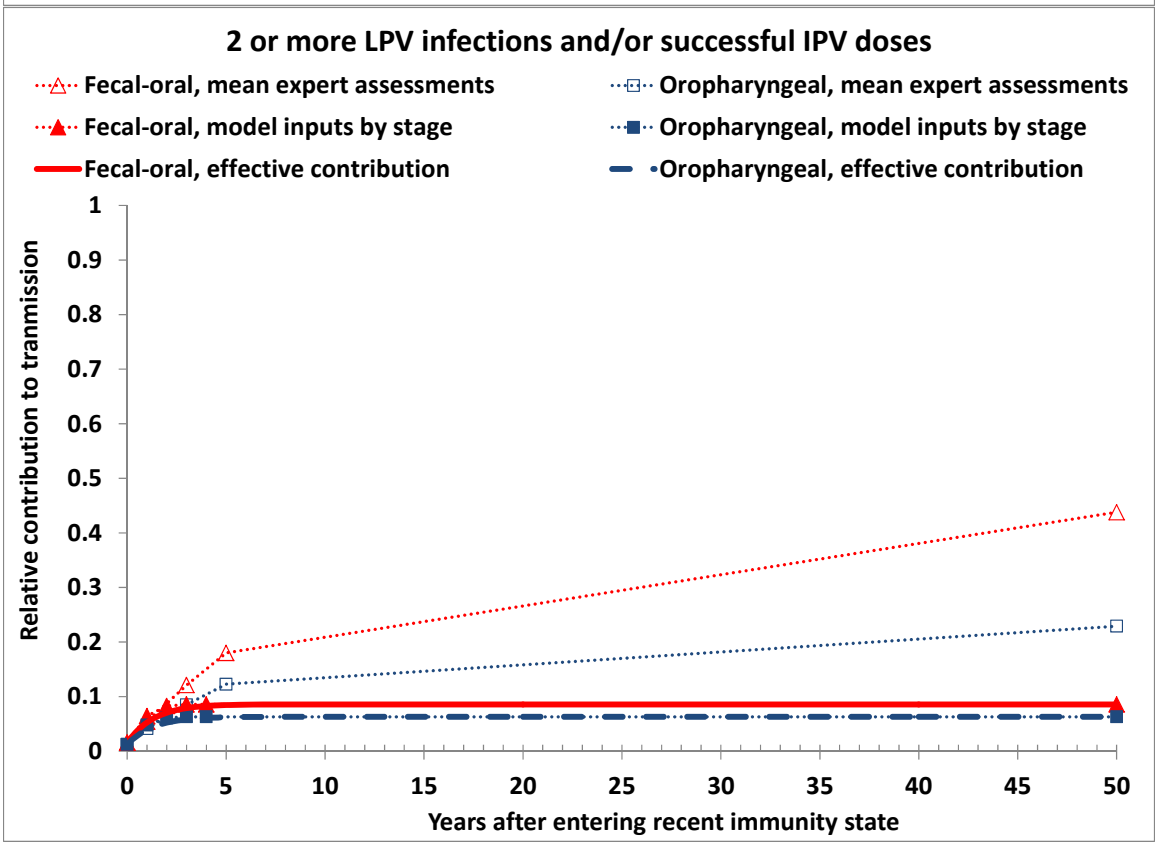

Figure A4 shows both the results of the multistate process for τ (i.e., relative R_0 of OPV compared to homotypic FRPV and WPV) and PIR as a function of the age of the virus and the inputs by discrete reversion stage that lead to these curves (dots indicate the values of the 20 reversion stages). With respect to τ, for which we assumed a linear increase in input values by reversion stage, we see that the multi-stage process leads to a more gradual approach to the maximum input, which occurs due to the dispersion of values as viruses progress through the stages. The true relationship for τ remains uncertain, and the model calibration focused on determining the correct effective average input values (i.e., by changing the assumptions about the shape and time to last stage) that produce behavior consistent with the known behavior of VDPVs. With respect to the PIR, curves similarly show differences between the results and input values, which again reflect dispersion that occurs due to the multistage process. In this case, the curves look different due to the assumed S-shaped function for PIR and the application of the log transformation after averaging the natural-scale PIR for each model stage. The effective input values represent the PIR of a virus ingested at the given viral age since OPV dose administration (i.e., the evolution time). Importantly, although we assume the lowest PIR for type 1 OPV, PIR becomes greater for type 1 than type 3 by approximately 85 days and greater than the type 2 PIR by approximately 32 days due to the greater PIR for FRPV type 1 than types 2 and 3 (Table I).

Figure A4: Assumed effect of reversion on basic reproductive number (R_0, top panel), and paralysis-to-infection ratio (*PIR*; bottom panel) of oral poliovirus vaccine-related viruses

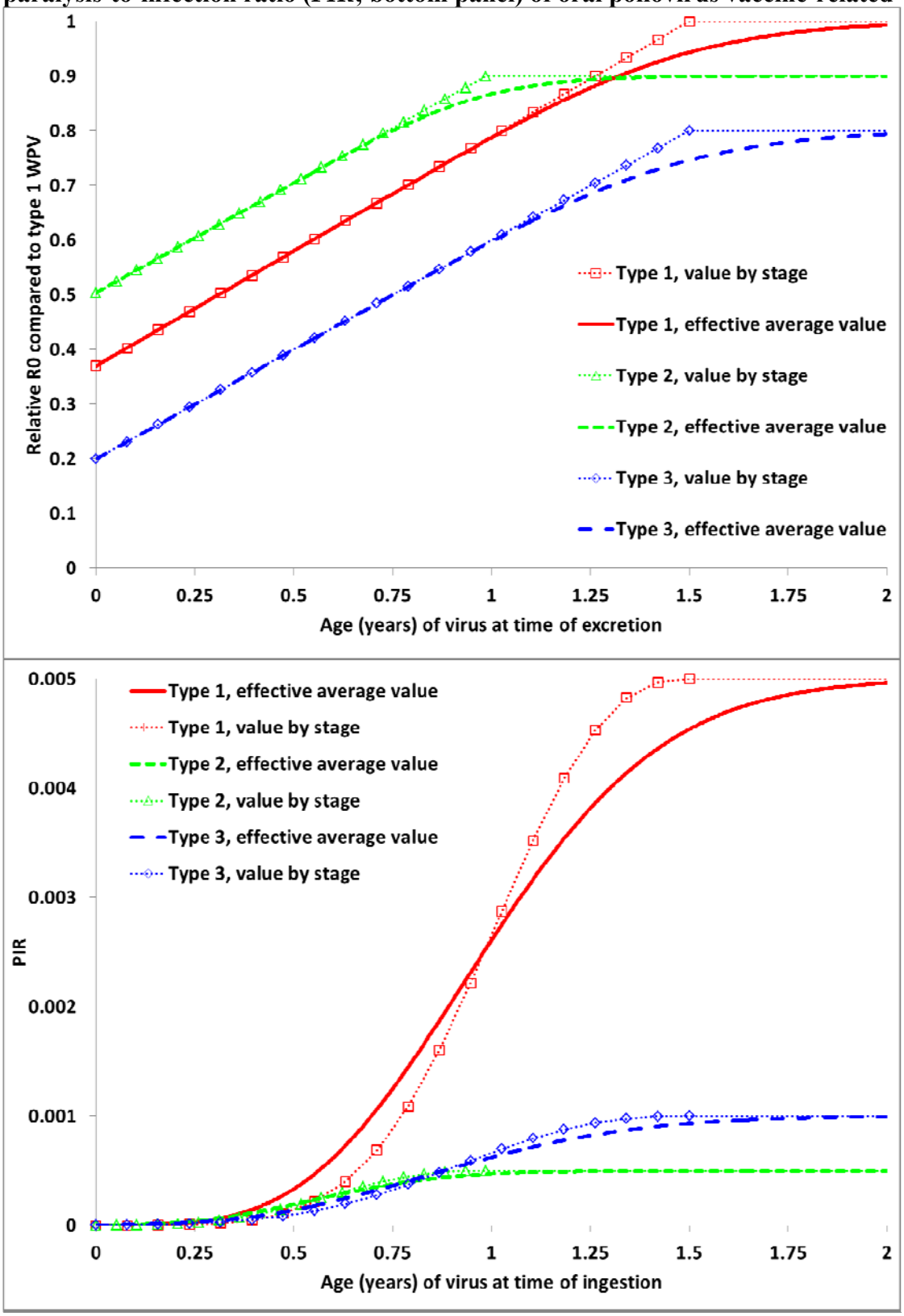

A3. Calculation of effective mortality rates

In all situations, we calculate the effective mortality rates μ_a based on the UN-estimated age distributions, following the same approach as previously described.[6] Briefly, we first linearly interpolate 5-year estimates from the UN[7] to obtain annual numbers by the situation-specific model age groups. For smaller situation-specific age groups than the five-year-wide age groups provided in the data,[7] we estimate numbers proportional to the width of those situation-specific age groups. We then determine the μ_a that exactly reproduce the annual numbers by situation-specific age group using the expressions in Duintjer Tebbens et al. (2011).[6]

In the event of situation-specific age groups of less than five years in width, we calculate a constant single μ for all situation-specific age groups within a five-year bracket. For example, we calculate one μ for all under-fives based on the changes in the under-five population in the UN data, and then apply this same μ for all situation-specific age groups under age five years (e.g., 0-2, 3-11 months, 1, 2, 3, and 4 years all receive the same under-five μ). Although this simplification leads to a small error in population size, we do not believe that the data (by five-year age groups) support estimates of μ values by smaller age groups. Given the small sample sizes, estimating μ for narrower age groups (e.g., 0-2 months) leads to very noisy and erratic results that reflect an artifact of attributing population size proportional to the width of these age groups rather than any realistic changes in μ values. We use effective birth rates based on surviving infants to account to some extent for the real difference in death rates between young infants and children aged 1 to 5 years.

Due to emigration or immigration, changing population registries and borders in some places, and/or inaccuracies in population estimates, in some instances we use negative μ_a values to reproduce the population estimates. In those instances, the model implicitly adds people to each stock in proportion to the number of people in that stock at the given time, thus providing a somewhat unbiased method to introduce people to the model to match the estimated population sizes by age group over time.

A4. Time series inputs

This section provides values of model inputs regarding vaccination that change over time in graphical form. Demographic data also represent time series inputs from publicly available data.[7] For The Netherlands, Table V already includes all information on vaccination coverage assumptions over time, and for Cuba, we assume the same coverage for each round and directly adopt the target age groups as listed in Más Lago (1999)[8] (as noted in Table VIII).

USA

Figure A5 shows the assumed annual cumulative coverage with IPV administered in campaigns to people under 20 years of age. For older individuals, we assume a fraction of 0.55 of this cumulative coverage (Table IV). The right axis shows the corresponding number of doses administered as a result of both IPV campaigns and routine IPV use (assumed to start in 1958, see Figure A6), compared with the reported number of doses distributed according to Morris et al. (1967)[9] and converted to administered doses by assuming 16% wastage.[10] Figure A6 shows the assumed routine coverage with 3 or more polio doses, and the assumed coverage with 1 or 2 doses for those assumed to receive fewer than 3 doses. We linearly interpolate between prior estimates[10] for 1987 and 1990 in the absence of good estimates for those years.

Figure A5: Assumed annual cumulative coverage of IPV campaigns in the USA, and corresponding doses administered (including from routine vaccination from 1958 forward), compared to estimated doses administered based on Morris et al. (1997)[9] with 16% wastage[10]

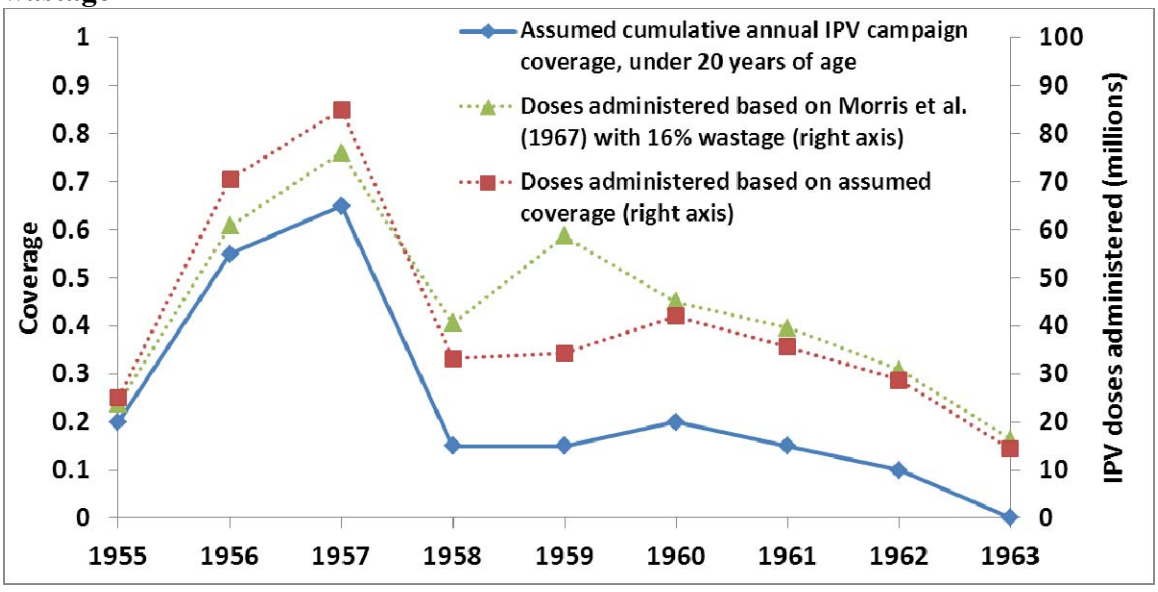

Figure A6: Assumed routine coverage with 3 or more polio doses in the USA, and with 1 or 2 doses given fewer than fewer than 3 doses, based on prior work[10] and DTP1 vs. DTP3 coverage,[11] respectively.

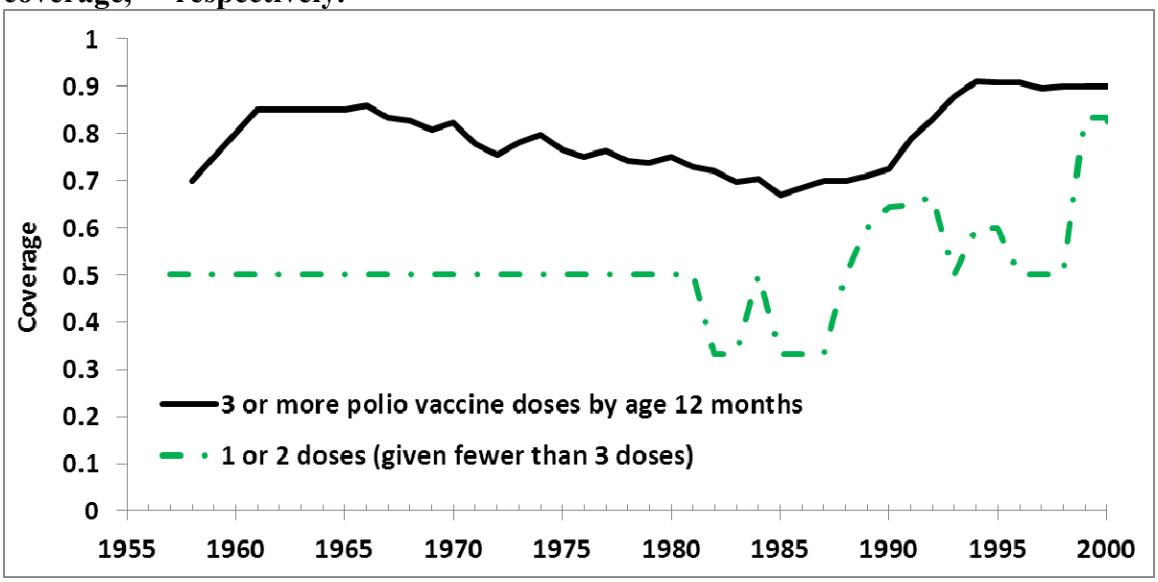

Albania

Figure A7 shows the assumed coverage for the isolated, under-vaccinated sub-population in the Albania model. For the years 1960-1977, coverage represents the fraction of 3-18 months olds receiving mOPV1 or a mix of all three monovalent vaccines in a given round.[12] We assume much lower coverage than the reported administrative coverage[12, 13] to account for long periods between campaigns due to irregular supply,[13] below-average coverage in the subpopulation, and/or poor vaccine take due to cold chain failures. For the years 1978-1996, coverage represents the fraction of children receiving all 3 primary doses by age 12 months. We assume 90% of the administrative coverage data to account for over-reporting in general and/or lower coverage levels in the subpopulation. As per Table VI, we assume booster doses occur at 18 months of age and attain 50% of the coverage with 3 doses, and from 1982 on we add another booster dose with the same coverage at 5 years of age.

Figure A7: Routine coverage assumptions for Albania, based on available data[11-13] and model calibration to characterize the under-vaccinated subpopulation.

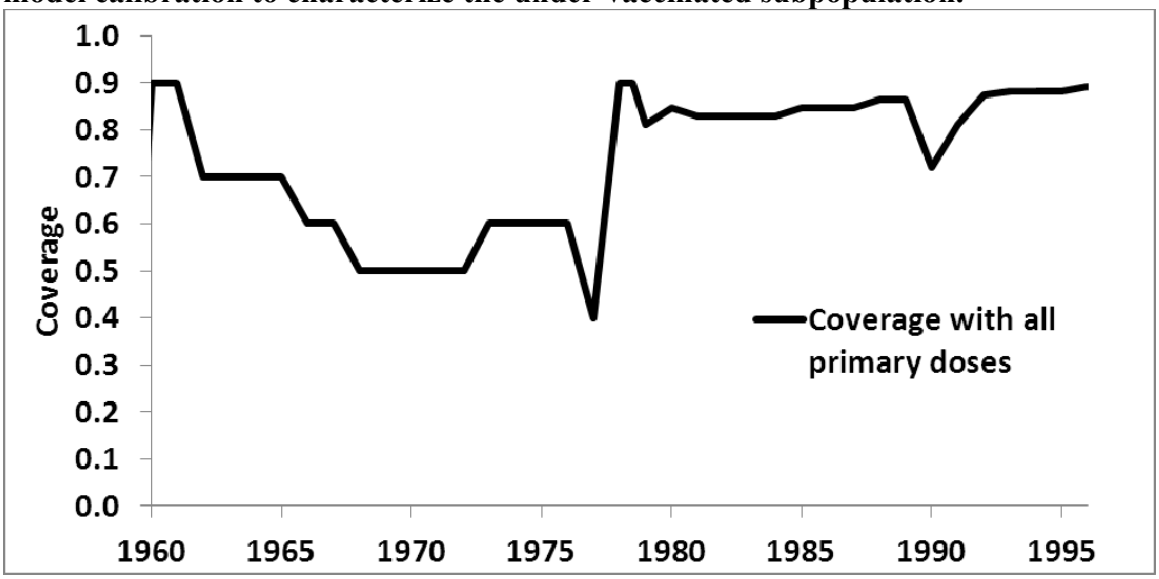

Tajikistan

Figure A8 shows the routine coverage assumptions for Tajikistan, including the coverage with the birth dose, coverage with 3 or more primary non-birth doses, and partial coverage with 1 or 2 doses, given fewer than 3 doses. Until 1991, we assume 90% coverage with 3 doses, with no partial or birth dose coverage in the absence of data before Tajikistan became an independent nation. For the birth dose coverage, we first divide the BCG coverage in the 3 modeled sub-national regions measured during the 2007 survey (2006 birth cohort)[14] by the WHO-UNICEF-estimated national BCG coverage for 2006.[11] We then multiply the WHO-UNICEF-estimated national BCG coverage for all years 1992-2010 by this ratio to account for differences between national coverage and coverage for the 3 regions. For the non-birth full and partial coverage, we multiply the WHO-UNICEF-estimated national POL3 coverage[11] for the years 1992-2006 by the ratio of estimated coverage from the 2007 survey[14] and the 2006 WHO-UNICEF-estimated national POL3 coverage.[11] We assume that after 2006, all coverage values remain constant at the level estimated from the 2007 survey[14] until 2010. Finally, we multiply all coverage levels by 0.90 to correct for possible over-estimation of coverage in the surveys due to the exclusion of unregistered children (Table VII).

Figure A9 shows the assumed timing and impact of SIAs conducted in Tajikistan prior to 2010, with the dates based on data reported to WHO (Gacic-Dobo, 2009, personal communication). We assume all SIAs targeted the 3 regions affected by the outbreak with tOPV, and that the (S)NIDs in 1995, 1996, and 1999 targeted 0-4 year olds, while all other (S)NIDs targeted 0-3 year olds. The height of the bars in Figure A9 show the assumed effective per-round impact (ζ), which translate to annual cumulative percentages of missed children of 20%, 20%, 15%, 10%, 10%, 15%, 25%, and 30%, during each year from 1995 to 2002, respectively.

Figure A8: Routine coverage assumptions for Tajikistan, based on available data.[14, 15]

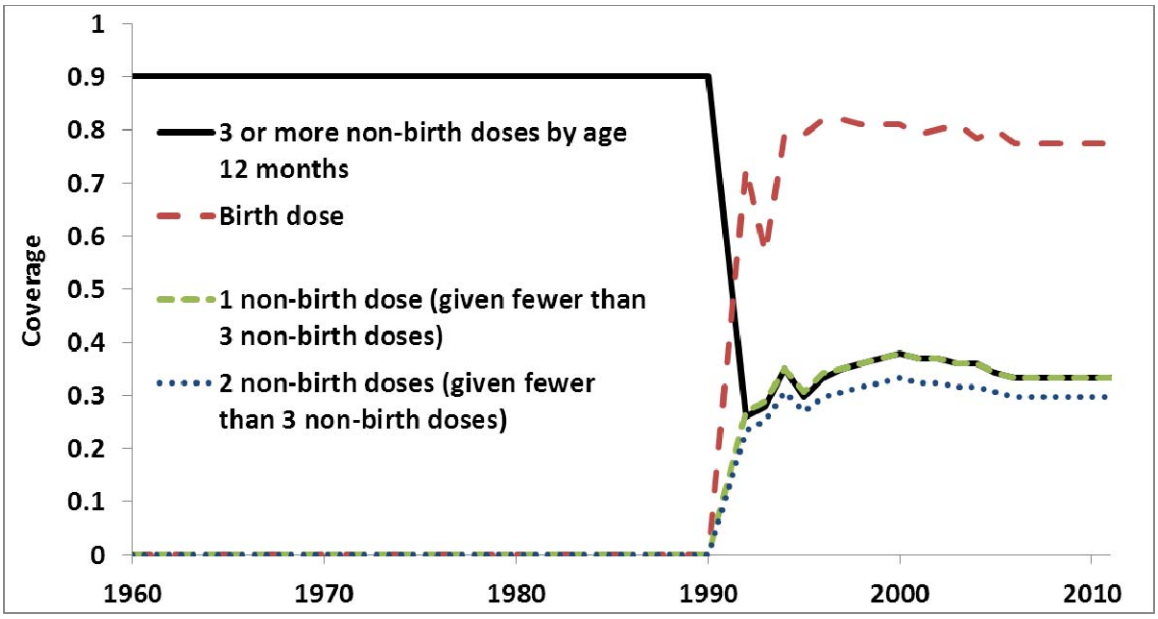

Figure A9: SIA assumptions for Tajikistan during the run-up, based on data reported to WHO (see Table VII for 2010 outbreak response assumptions)

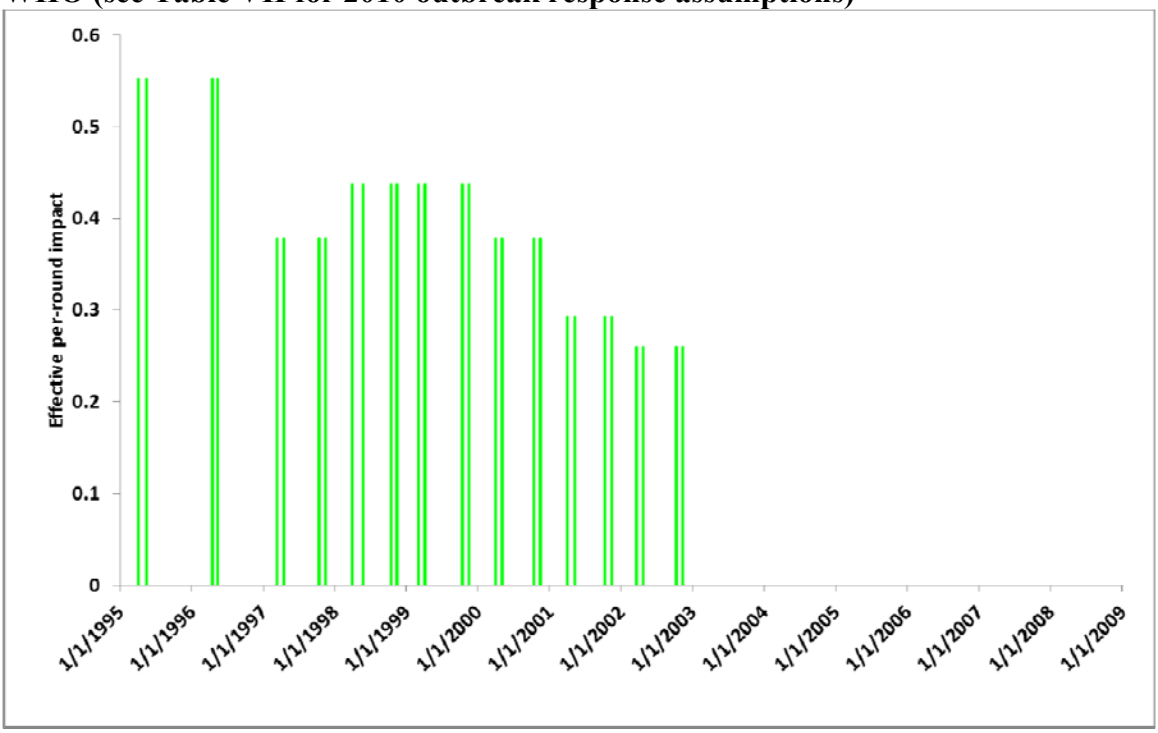

Haiti

Figure A10 shows the routine coverage assumptions for Haiti, based on linear interpolation between results from DHS surveys conducted in 1994-1995, 2000, and 2005-2006[16] (and applied to the birth cohorts of the preceding years). For the years 1980 (i.e., the assumed beginning of routine tOPV use) to 1992 (i.e., the last birth year before the first survey), we multiply the WHO-UNICEF-estimated coverage[11] for that year by the ratio of each of the four coverage values (i.e., birth dose, 3 or more doses, 1 dose given fewer than 3 doses, 2 doses given fewer than 3 doses) from the 1994-1995 survey to the WHO-UNICEF-estimated POL3 coverage for 1993.[11] Figure A11 shows the assumptions about the SIAs conducted in Haiti prior to the outbreak in 2000-2001, based on very limited data.[17, 18] We assume that all SIA targeted 0-4 year old children in the entire country with tOPV and involved two rounds on days 50 and 120 of each year (Table IX). The effective per-round impacts in Figure A11 translate to annual cumulative percentages of missed children of 36%, 16%, 4%, 1%, 1%, 4%, 9%, 16%, 16%, and 16%, during each year from 1986 to 1995, respectively.

Figure A10: Routine coverage assumptions for Haiti, based on available data.[11, 16]

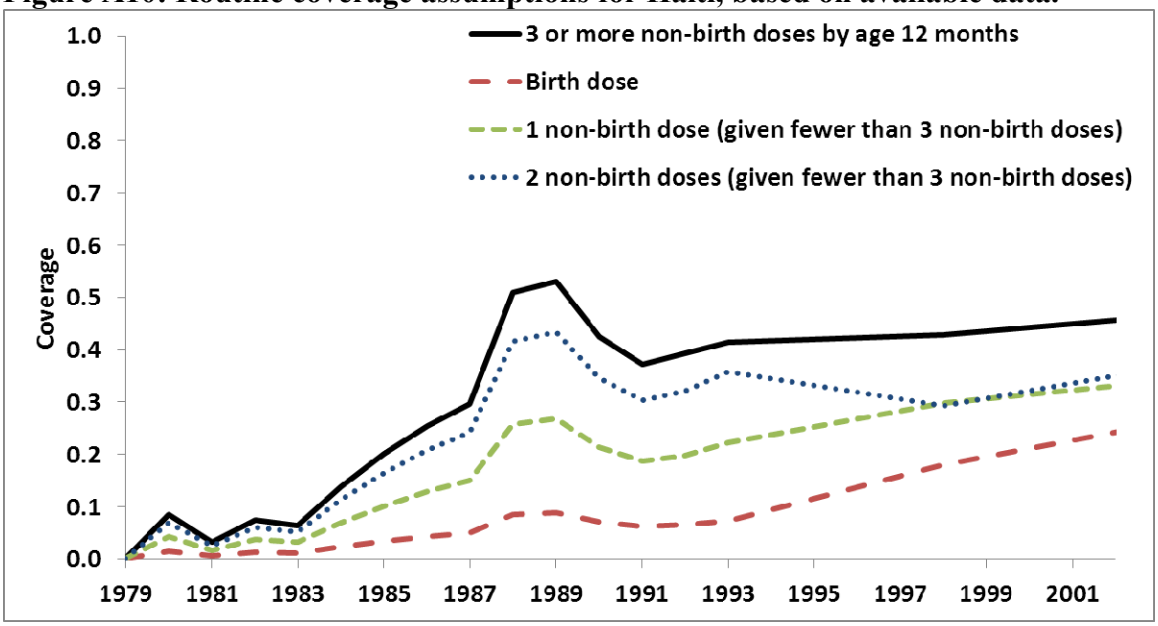

Figure A11: SIA assumptions for Haiti during the run-up (see Table IX for 2001 outbreak response assumptions)

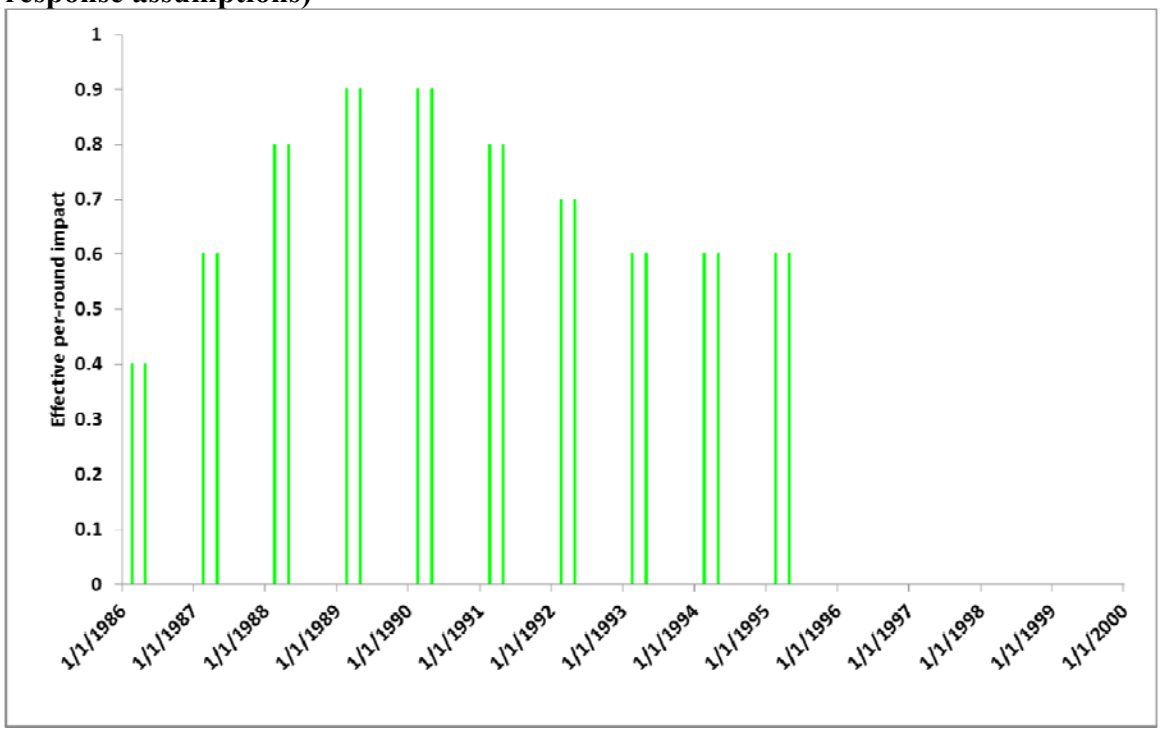

Madura

Figure A12 shows the routine coverage assumptions for Madura, based on WHO-UNICEF-estimated coverage for Indonesia from 1981 to 2001.[11] This may provide an overestimate for the modeled rural subpopulation of Madura, but remains of relatively little consequence given that population immunity comes primarily from WPV transmission and SIAs conducted intermittently from 1995 to 2002. From 2002, we assume constant coverage using the values reported from a convenience sample of the children under 5 years of age in communities affected by the outbreak.[19] The raw data (Estívariz, 2012, personal communication) provide a basis for estimating partial coverage with 0, 1, 2 or 3 doses given fewer than 4 doses, which we apply without changes over time to all years. Consequently, Figure A13 shows only the coverage with all 4 primary doses by age 12 months. Figure A13 shows the assumptions about the SIAs conducted in Madura prior to the outbreak in 2000-2001, based on data reported to the WHO. We assume that not all SNIDs reached the rural subpopulation and that all SIAs targeted 0-4 year old children in the entire rural subpopulation with tOPV and involved two rounds on days 240 and 280 of each year (Table X). The effective per-round impacts in Figure A11 translate to annual cumulative percentages of missed children of 4% from 1995-1998 and 9% in 2000 and 2002.

Figure A12: Routine coverage assumptions for Madura, based on available data.[11, 19]

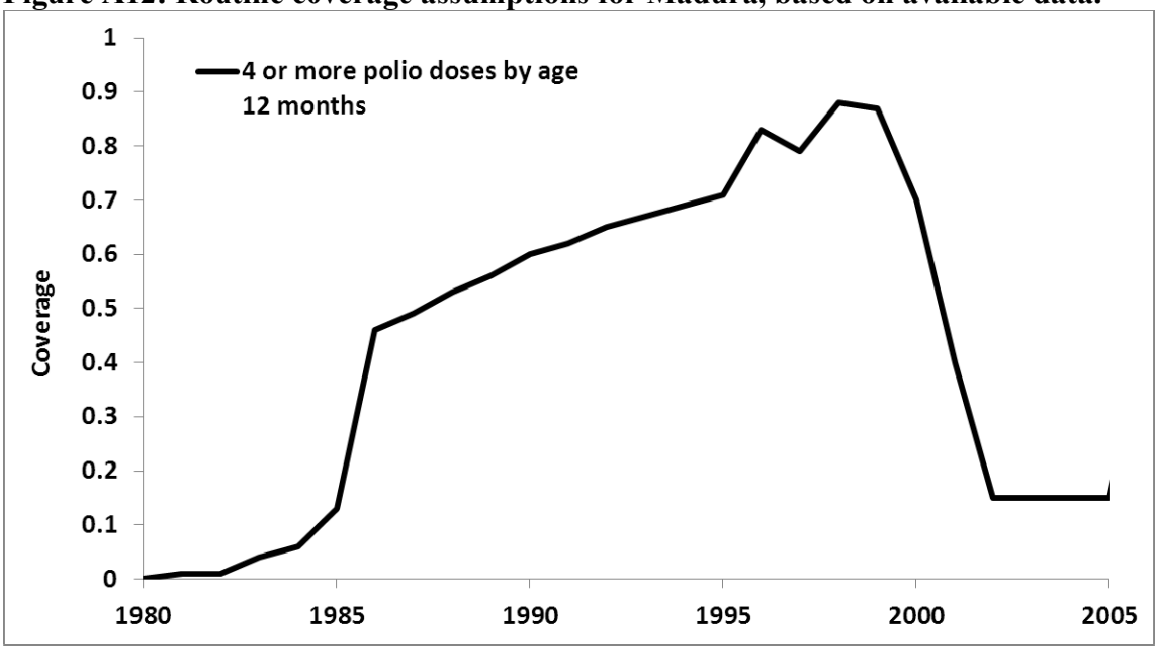

Figure A13: SIA assumptions for Madura during the run-up (see Table X for 2005 outbreak response assumptions)

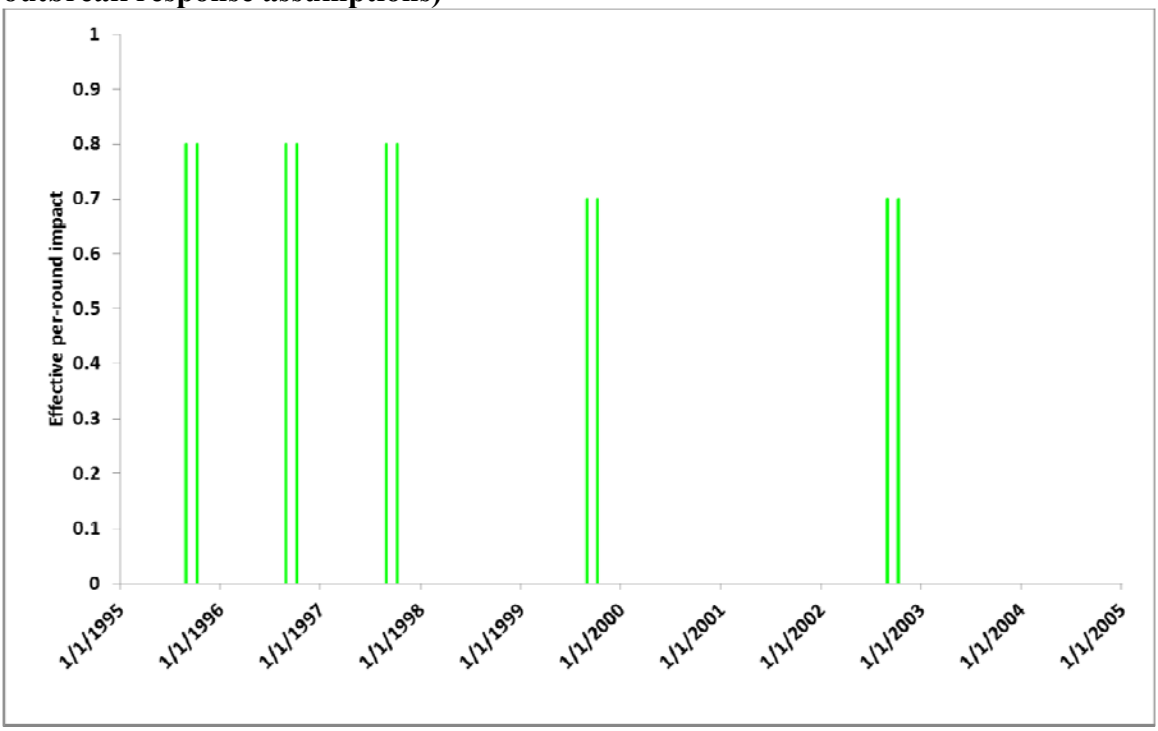

Northern Nigeria

Figure A14 shows the routine coverage assumptions for northern Nigeria. We linearly interpolate between DHS surveys conducted in 1990, 1999, 2003, and 2008,[20] which include birth dose coverage, coverage with the third non-birth dose (POL3), and partial coverage, and provide results for each geopolitical zone in Nigeria, including the northwest (NW). For the years 1984 (i.e., the assumed beginning of routine polio immunization program) to 1988 (i.e., the last birth year not covered by DHS surveys), we multiply the WHO-UNICEF estimated POL3 coverage[11] by the POL3 estimate from the 1990 DHS (covering the 1989 birth cohort) divided by the 1990 WHO-UNICEF-estimated POL3 coverage.[11] We assume that the birth dose and partial coverage increased proportionally to the POL3 coverage in those years. For 2008 and beyond, we assume the POL3 coverage increased at the same rate as the WHO-UNICEF-estimated POL3 coverage[11] using the 2008 DHS estimate[20] as the starting point, while we assume that the birth dose and partial coverage stayed constant at the level estimated from the 2008 DHS.[20] To maintain the approximate average coverage values for the entire NW zone in Figure A14, we multiply all coverage values by 1.08 for the general population and all coverage values by 0.29 for the under-vaccinated subpopulation.

Figure A15 shows the assumptions about timing, vaccine use, and the effective impact of the SIAs conducted in northern Nigeria, broken down by modeled subpopulation. Given that we know that many rounds, especially in recent years, did not target the entire NW zone, we account for the fraction of the NW zone targeted in each round, based on estimates of covered states. Thus, Figure A15 shows the product of the assumed effective per-round impact (ζ) and the targeted fraction. The assumptions in Figure A15 translate to the annual cumulative percentages of missed children shown in Figure A16. Figure A16a shows the breakdown by modeled subpopulation and the combined percentages (calculated as the sum over each subpopulation of the annual cumulative percentage of missed children multiplied by the relative size of the subpopulation compared to the NW). Figure A16b shows the breakdown by vaccines containing each serotype (e.g., by not including mOPV1 rounds in the missed children calculation for type 3), which clearly illustrates the large fraction of children that did not receive type 2 or type 3 containing vaccine during SIAs in 2008, which led to the subsequent large type 2 and 3 outbreaks.

Figure A14: Routine coverage assumptions for northern Nigeria, based on available data.[11, 20]

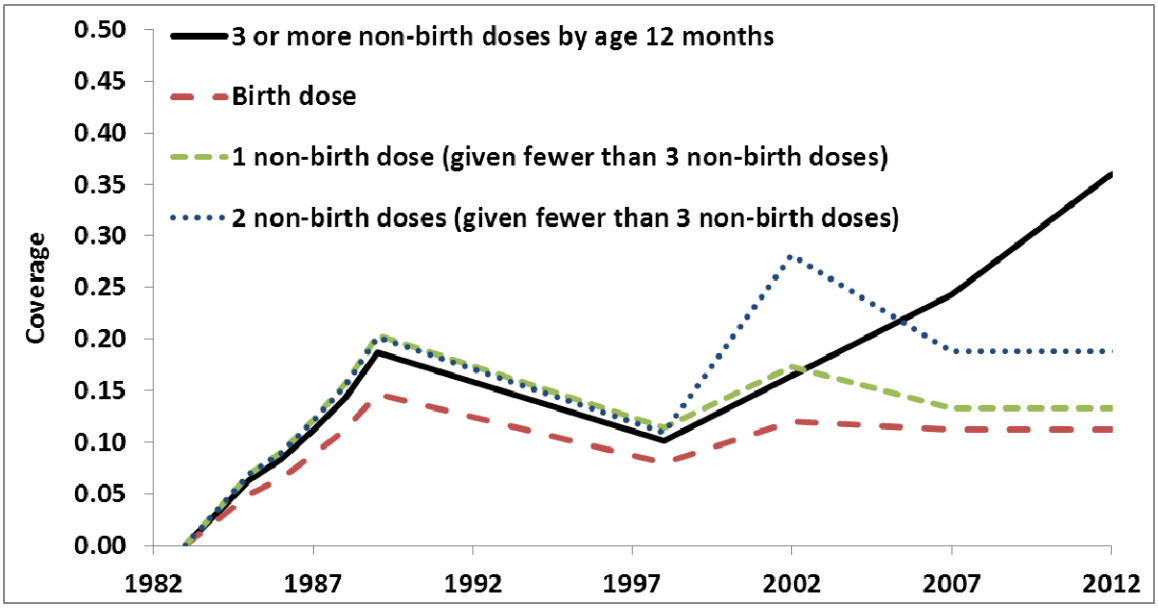

Figure A15: SIA assumptions for northern Nigeria, showing the product of the assumed effective per-round impact (ζ) and the assumed fraction of the NW zone targeted.

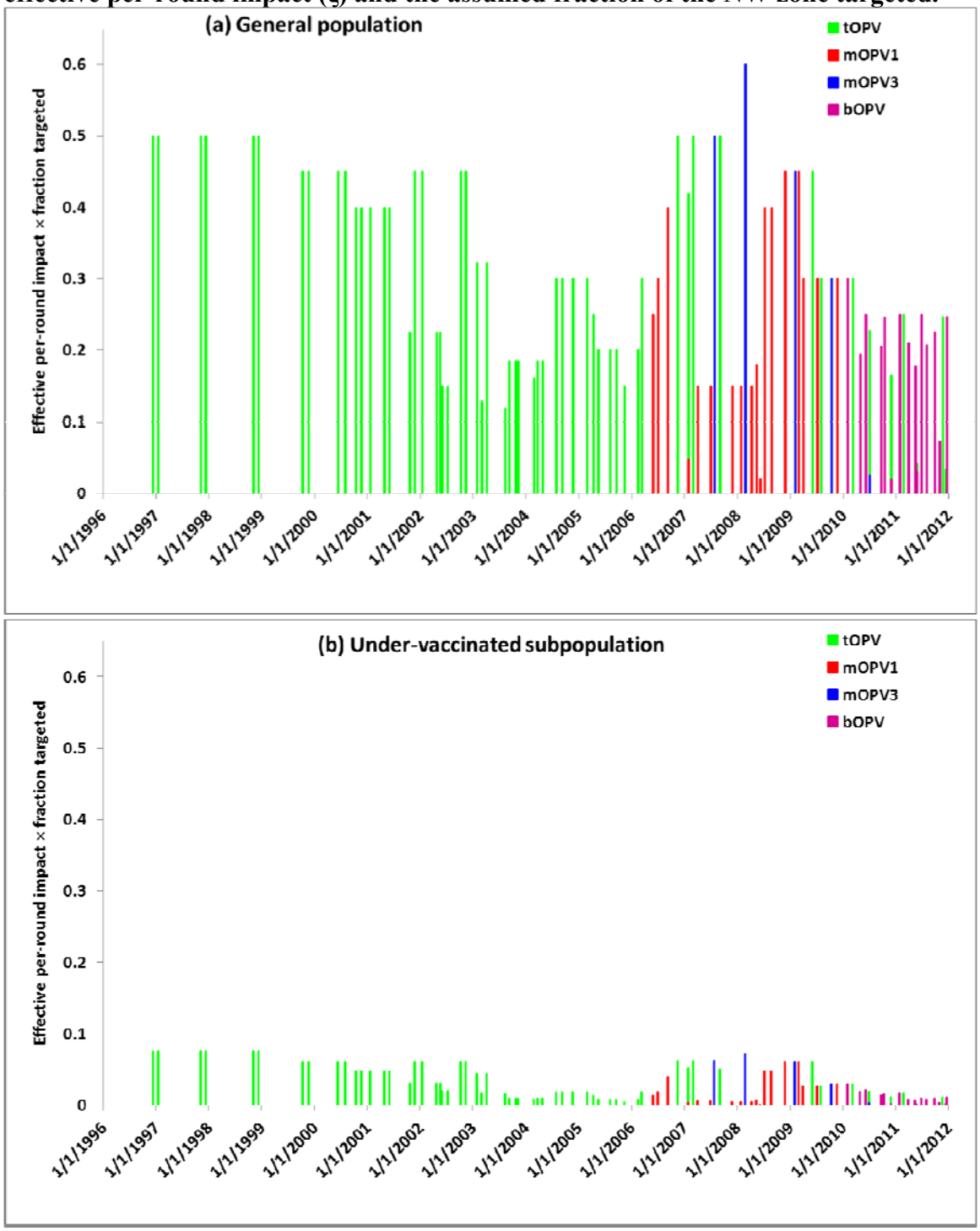

Figure A16: Annual cumulative percent of missed children by SIAs in northern Nigeria, corresponding to the assumptions in Figure A15.
(a) By (sub-)population (showing children missed by any OPV vaccine)

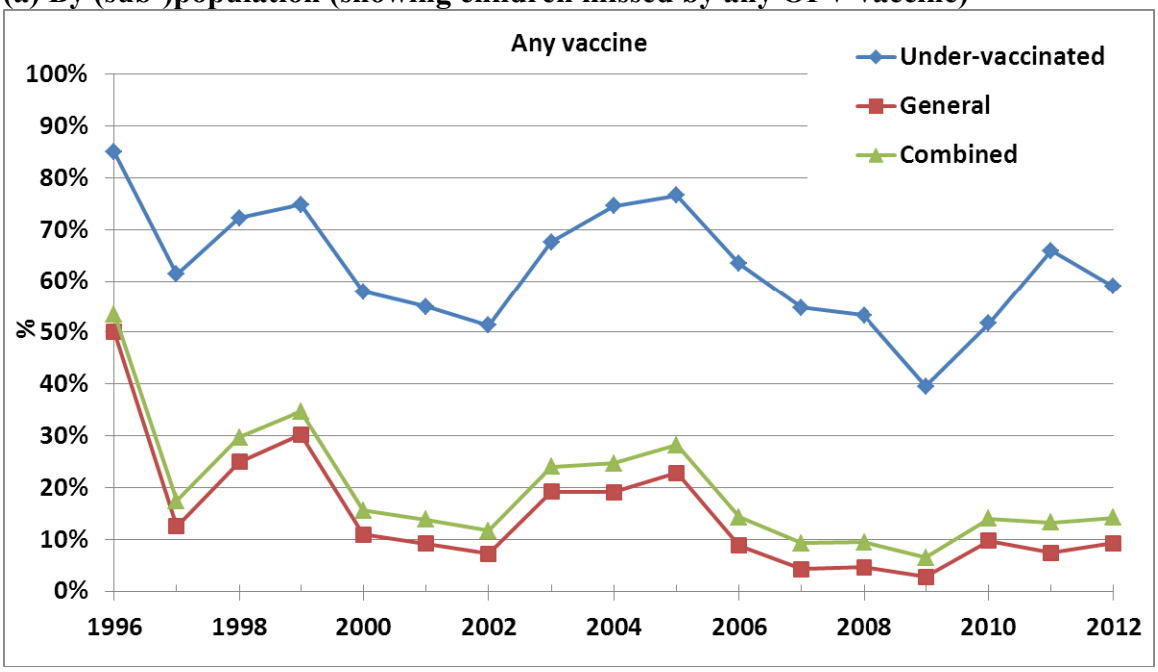

(b) By type-containing vaccines (showing the combined results for the two modeled subpopulations)

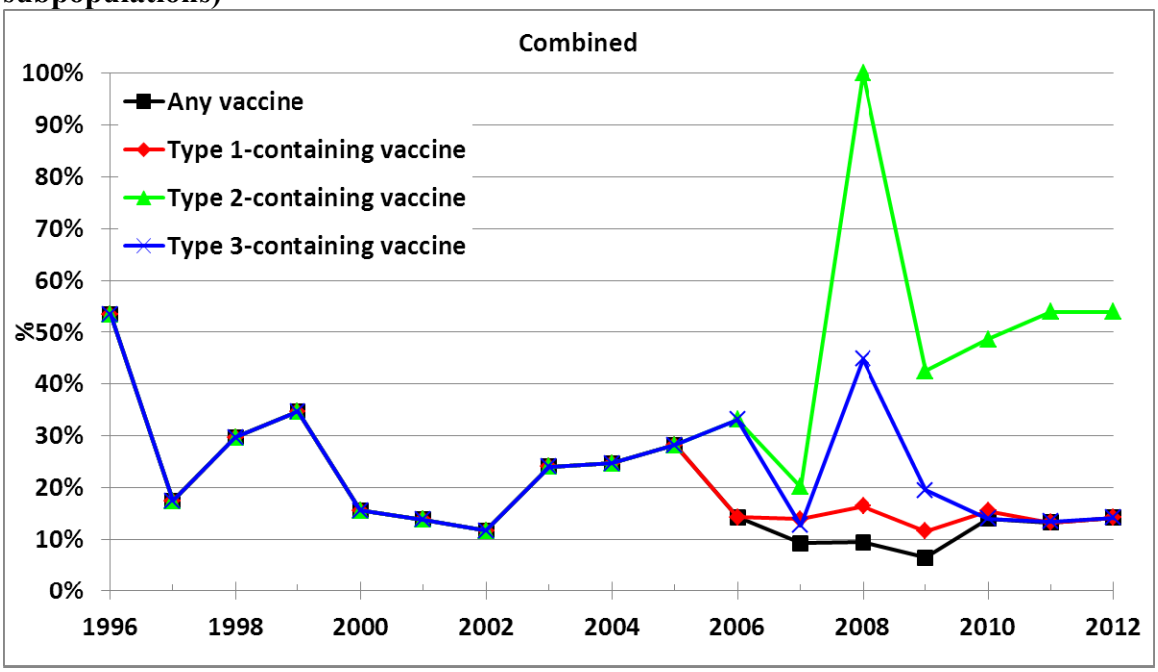

Northern India

Figure A17 shows the routine coverage assumptions for Bihar and WUP in northern India. We linearly interpolate between DHS survey results conducted in 1992-1993, 1998-1999, and 2005-2006[21] which include coverage with the third non-birth dose (POL3) and partial coverage by state. Only the 2005-2006 DHS reports coverage with the birth dose (POL0), and consequently we estimate the coverage with the birth dose by multiplying the POL3 estimate for a given year with the ratio of POL0 to POL3 estimates in the 2005-2006 survey (i.e., 0.37 in Bihar and 0.39 in WUP).[21] The DHS surveys[21] report a large gap between DTP3 and POL3 coverage coinciding with the beginning of SIAs in India, which suggests that POL3 coverage may include doses given during SIAs, but could also relate to DTP3 supply shortages. Given uncertainty about the two estimates, we assume the average coverage for DTP and POL for each dose. For the years 1980 (i.e., the assumed beginning of routine polio immunization program) to 1990 (i.e., the last birth year not covered by DHS surveys), we assume a linear increase from 0 to the levels estimated from the 1992-1993 survey,[21] and we assume constant levels after the most recent survey in 2005-2008.[21] We assume the same routine vaccination coverage levels for the under-vaccinated and the general population in WUP.

Figure A18 shows the assumption about timing and effective impact of the SIAs conducted in northern India, broken down by modeled subpopulation and color-coded by vaccine used in each round. As for northern Nigeria, Figure A18 shows the product of the assumed effective per-round impact (ζ) and the fraction of the region targeted. The assumptions in Figure A18 translate to the annual cumulative percentages of missed children shown in Figure A19. Figure A19a shows the breakdown by modeled subpopulation and the combined percentage for WUP (calculated as the sum over each subpopulation of the annual cumulative percentage of missed children multiplied by the relative size of the subpopulation compared to all of WUP). Figures A19b and A19c show the breakdown by vaccines containing each serotype, which as in northern Nigeria clearly illustrates the gap in use of type 3-containing vaccines from 2006 and led to the resurgence of type 3 cases in 2007-2009. However, unlike in northern Nigeria, despite the reduction in use of type 2-containing vaccine, a large type 2 cVDPV outbreak did not occur, consistent with the much better routine coverage.

Figure A17: Routine coverage assumptions for northern India, based on available data.[21]

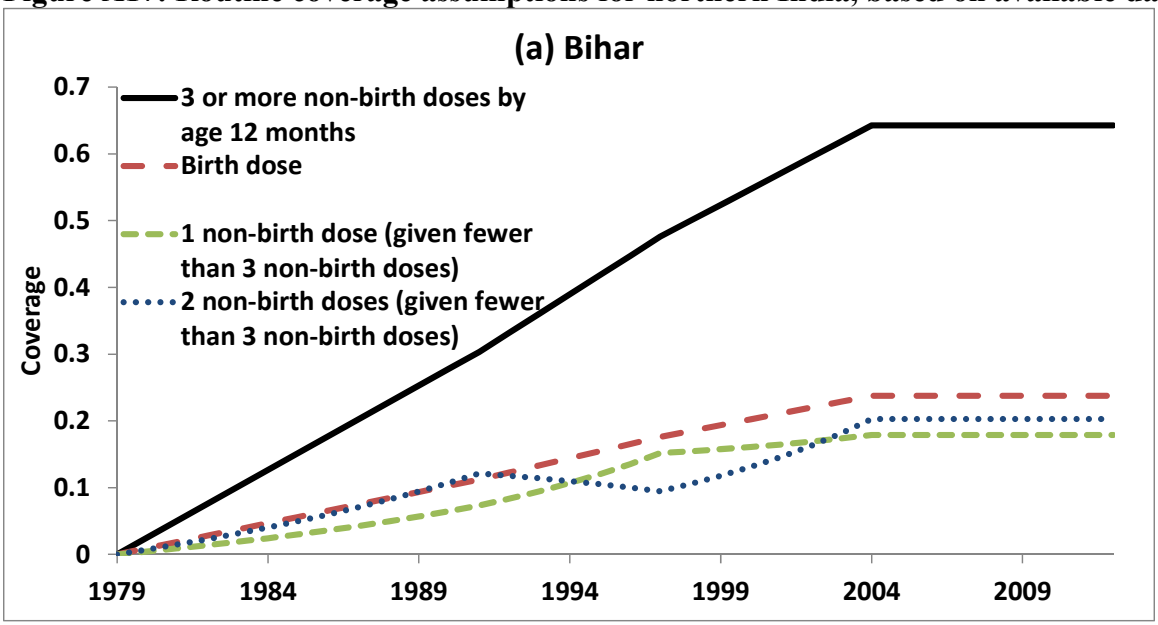

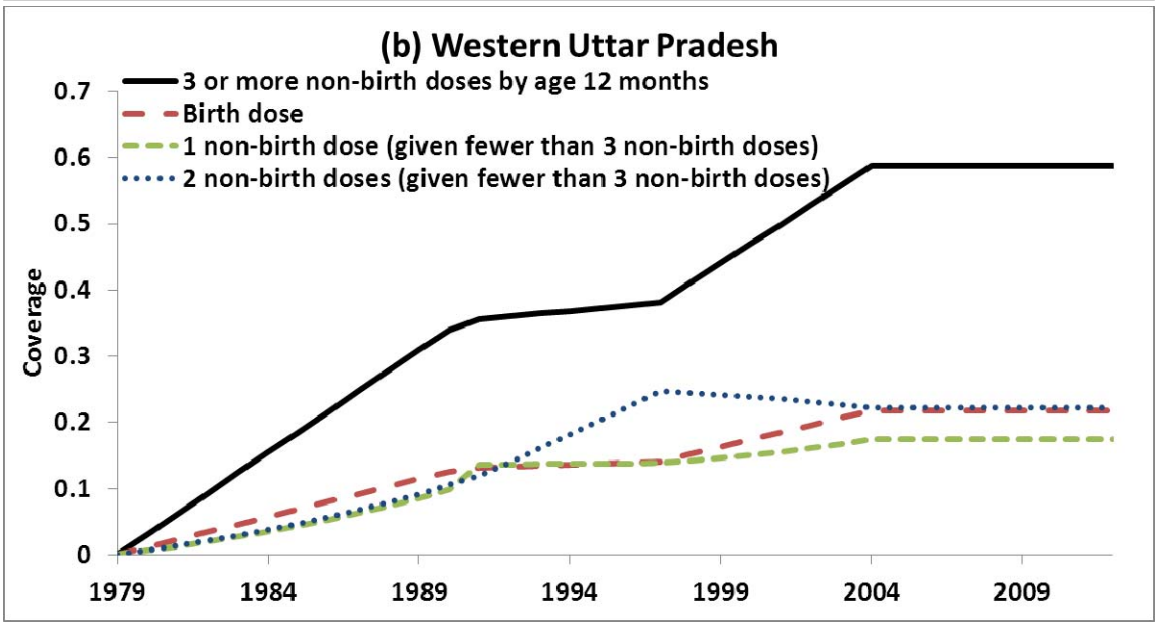

Figure A18: SIA assumptions for northern India, showing the product of the assumed effective per-round impact (ζ) and the assumed fraction of the region targeted.

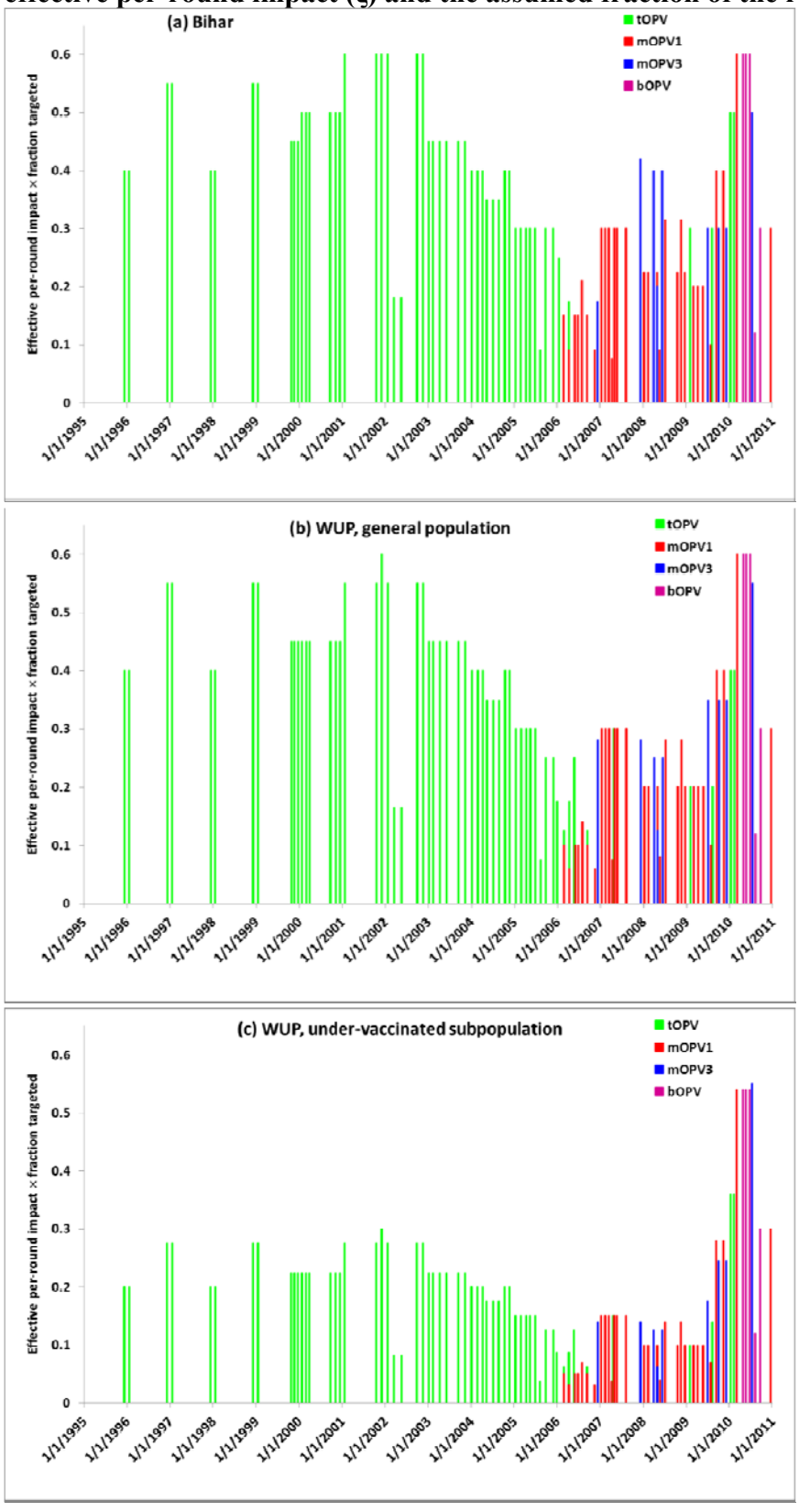

Figure A19: Annual cumulative percent of missed children by SIAs in northern India, corresponding to the assumptions in Figure A18.
(a) By (sub-)population (showing children missed by any OPV vaccine)

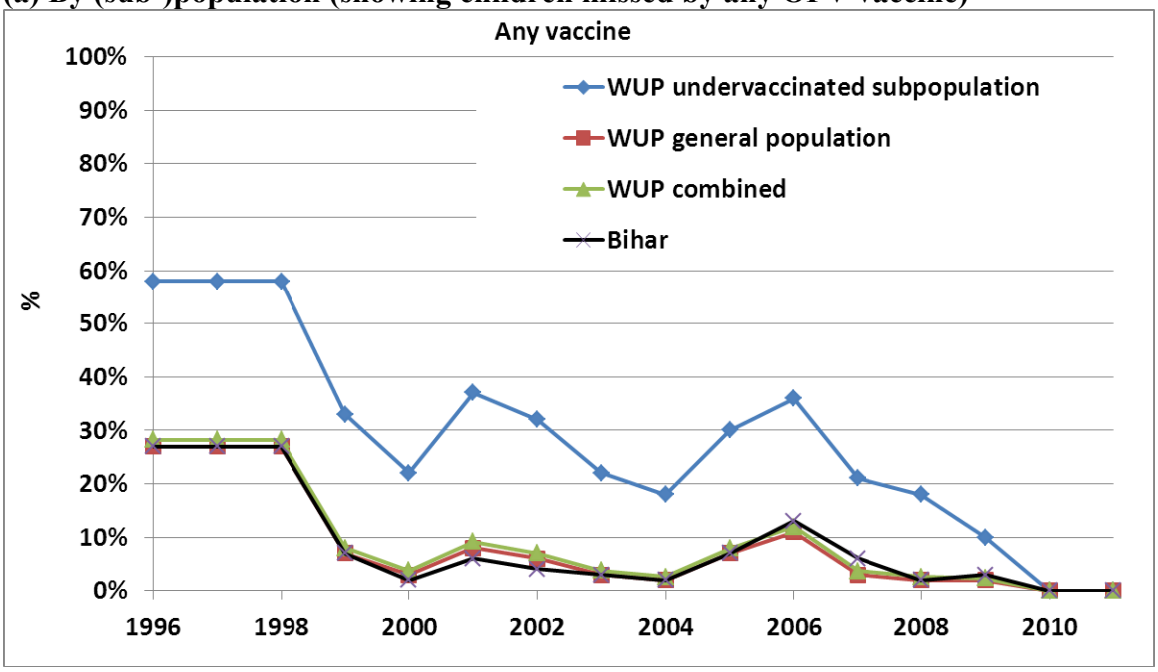

(b) By type-containing vaccines, in WUP (showing the combined results for the two modeled subpopulations in WUP)

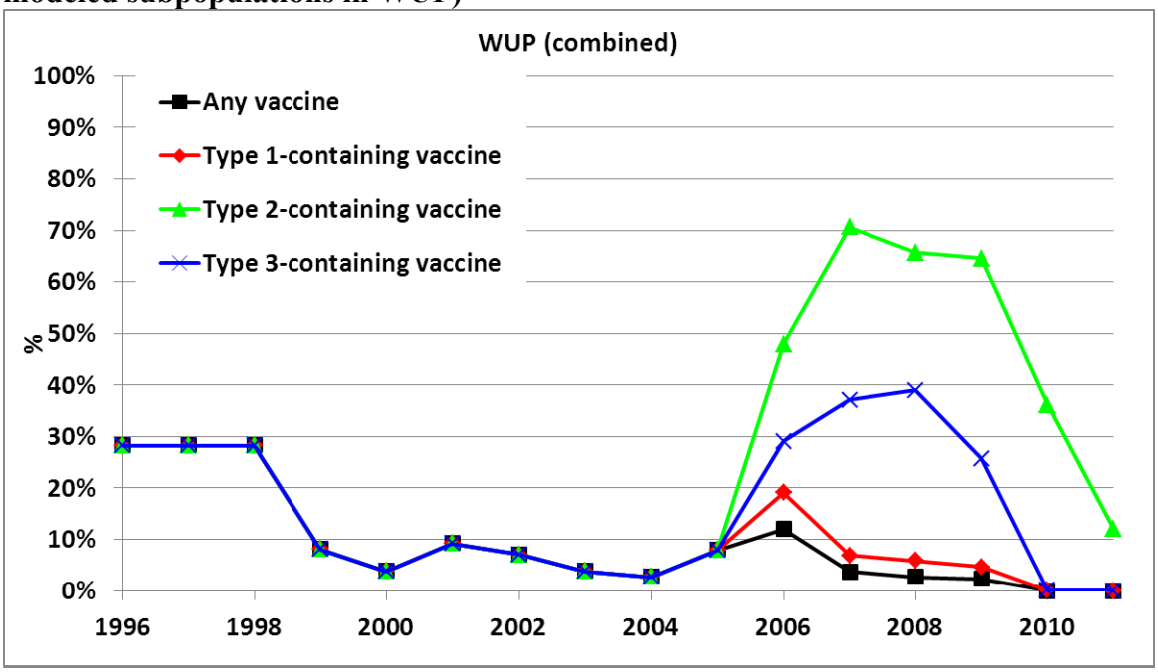

(c) By type-containing vaccines, in Bihar

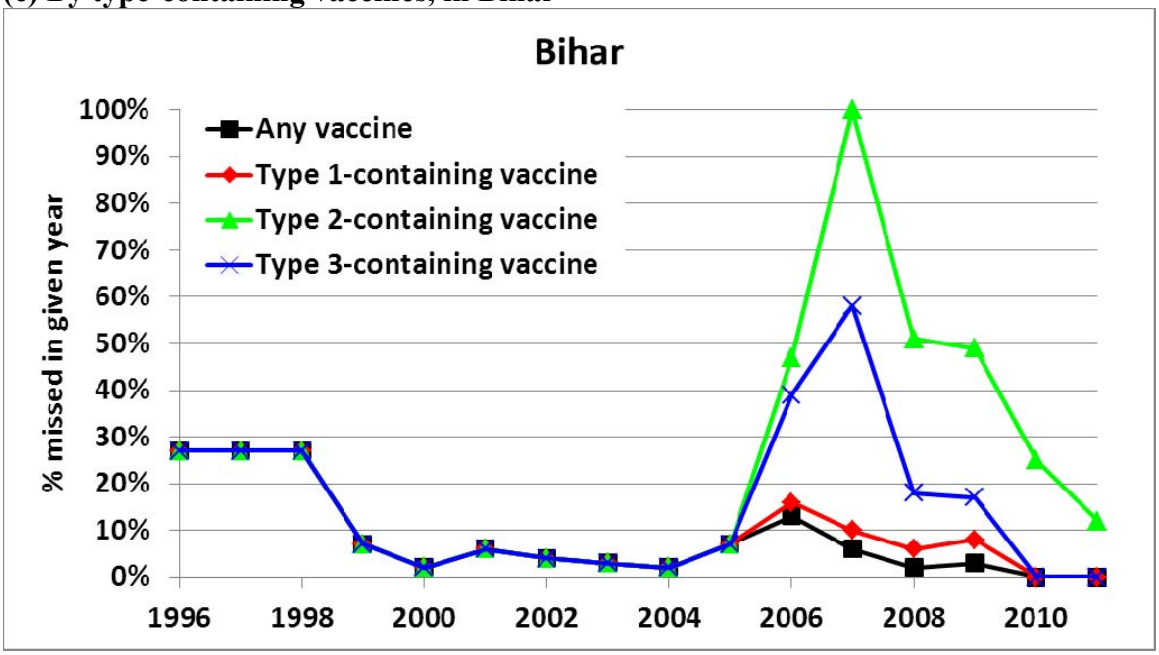

A5. Additional results

This section includes results of the models for different situations leading up to the time periods shown in the main paper figures, as well as further selected results of interest for the different situations.

The USA model already includes the model results and data going back out to 1948, before which we suspect significant underreporting. Figures A20-A27 show the run-ups for The Netherlands, Albania, Tajikistan, Cuba, Haiti, Madura, northern Nigeria, and northern India, respectively.

Figure A20: Run-up for The Netherlands (reported cases from van den Hof (1998),[22] and frequency of type 3 to total cases during 1953-1958 from Verlinde (1959)[23])

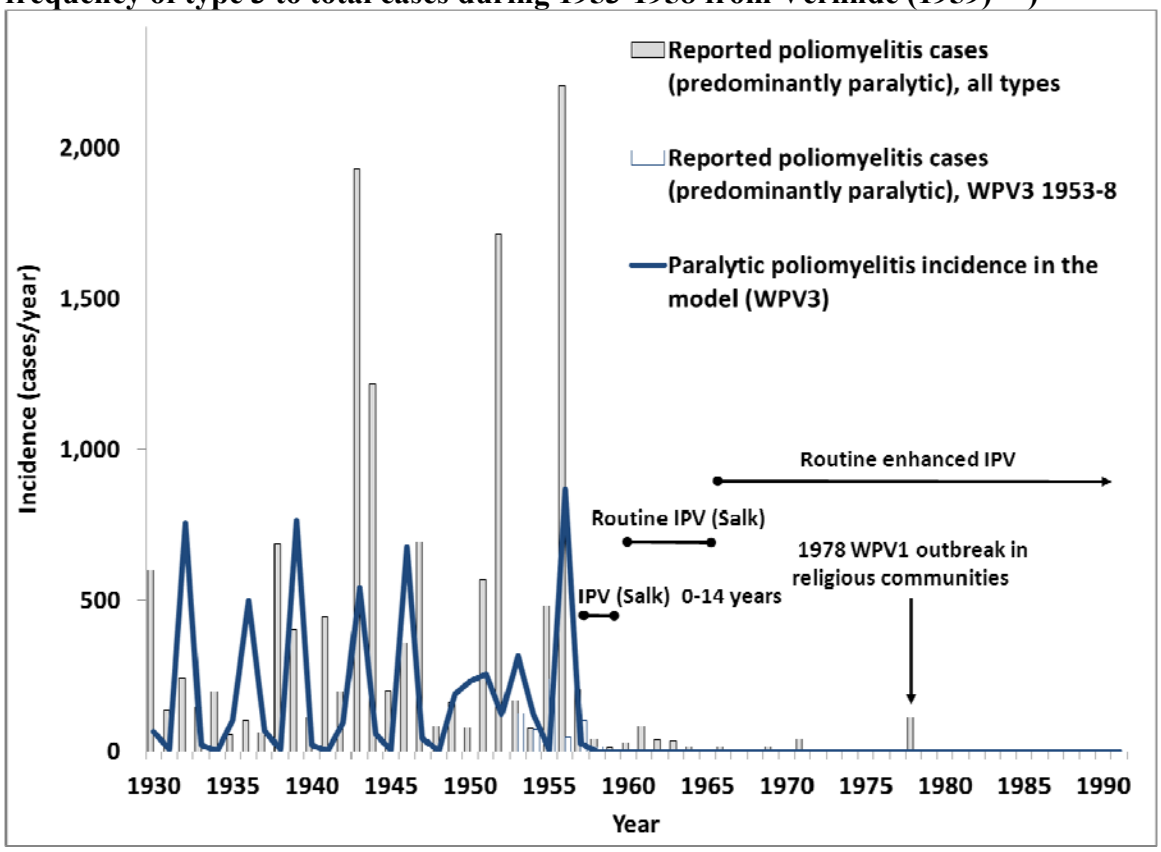

Figure A21: Run-up for Albania (reported cases starting in 1960 from Prevots et al. (1998)[12])

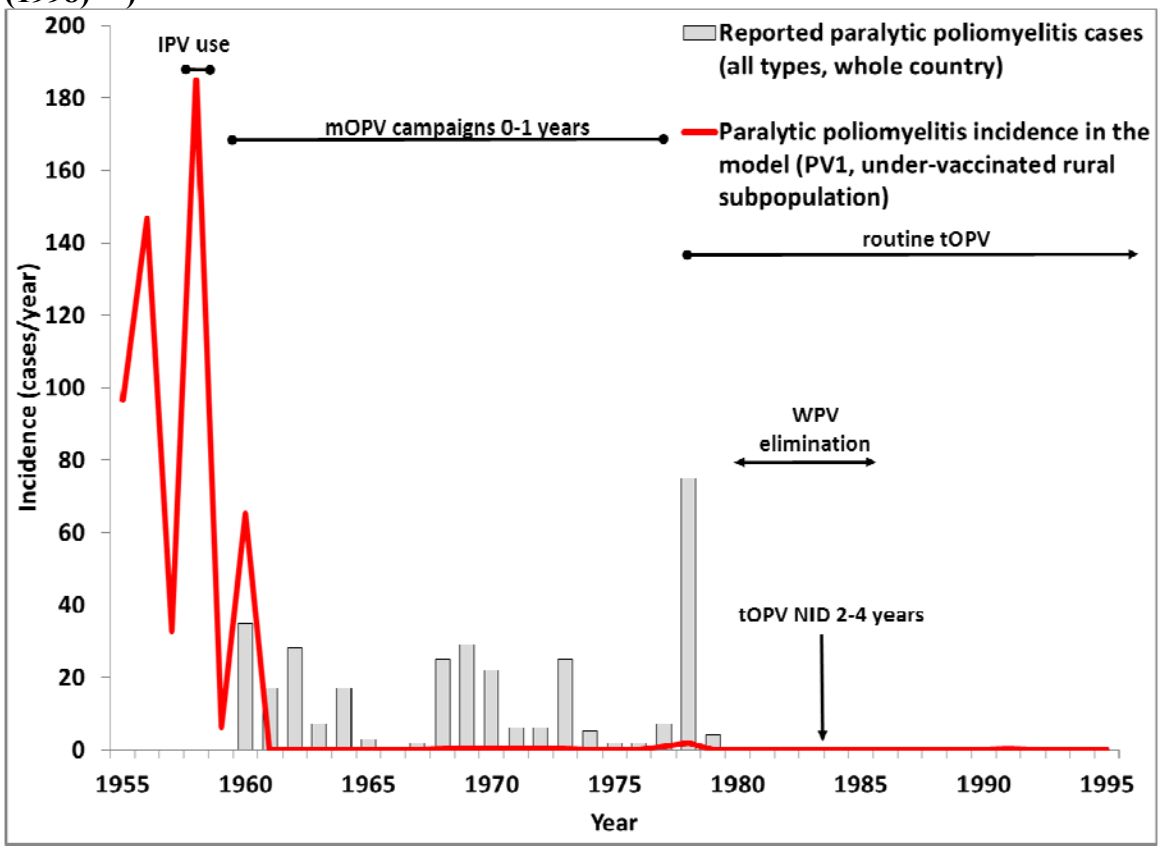

Figure A22: Run-up for Tajikistan (reported cases starting in 1991 from WHO (2012)[24])

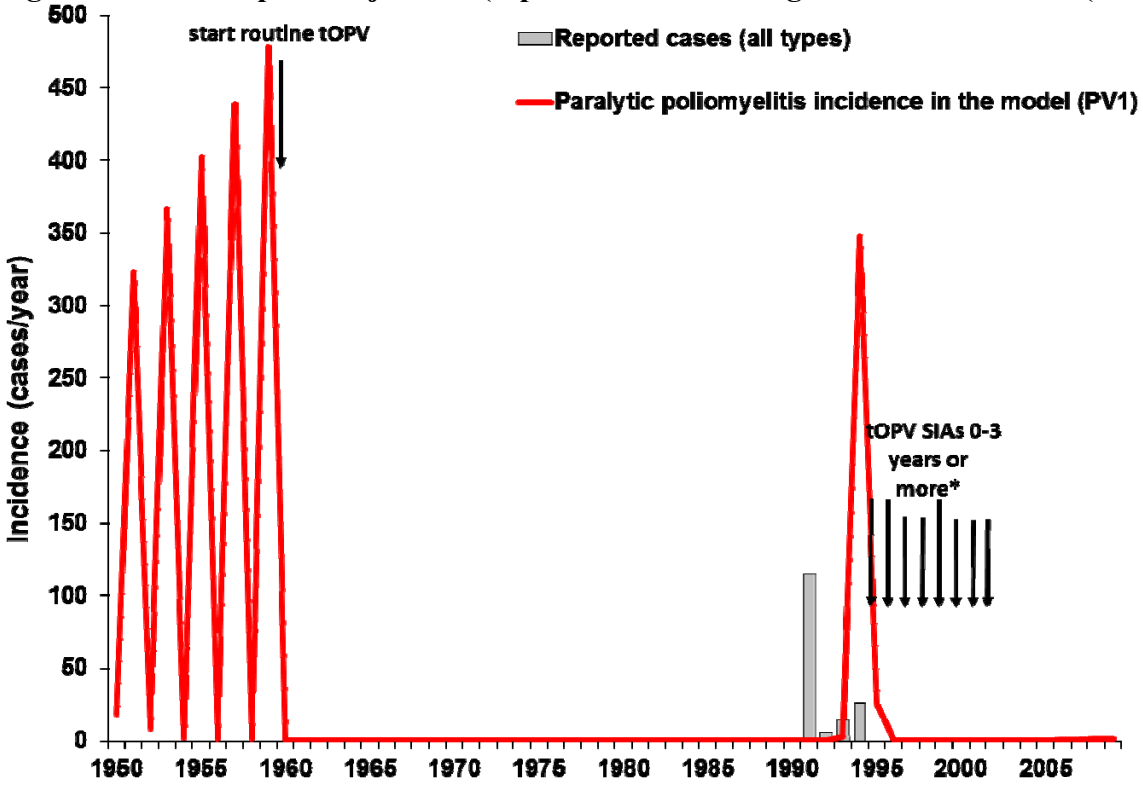

* One arrow represents a year with at least one SIA round. Shorter arrows represent SIAs that we assume targeted 0-3 year old children, longer arrows represent SIAs that we assume targeted 0-4 year old children

Figure A23: Run-up for Cuba (reported cases from Rodriguez-Cruz (1984)[25])

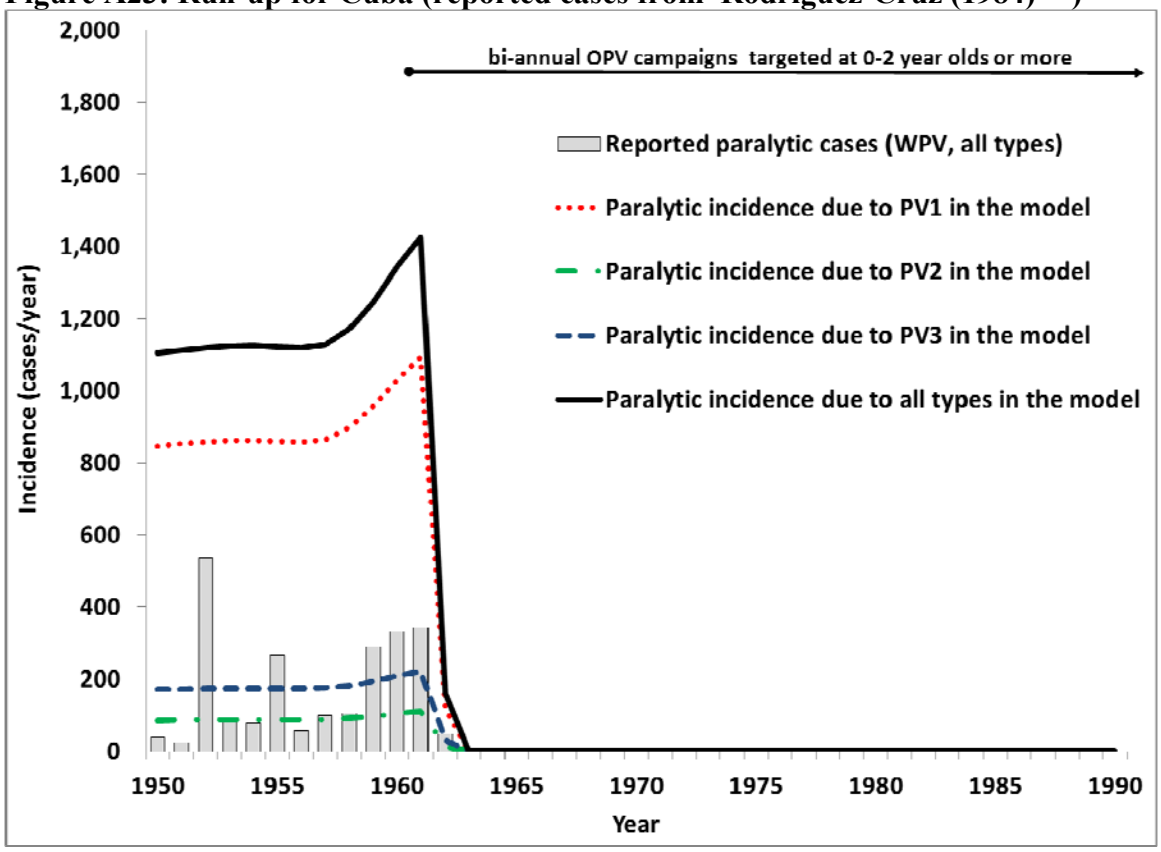

Figure A24: Run-up for Haiti (reported cases starting in 1980 from WHO (2012)[24])

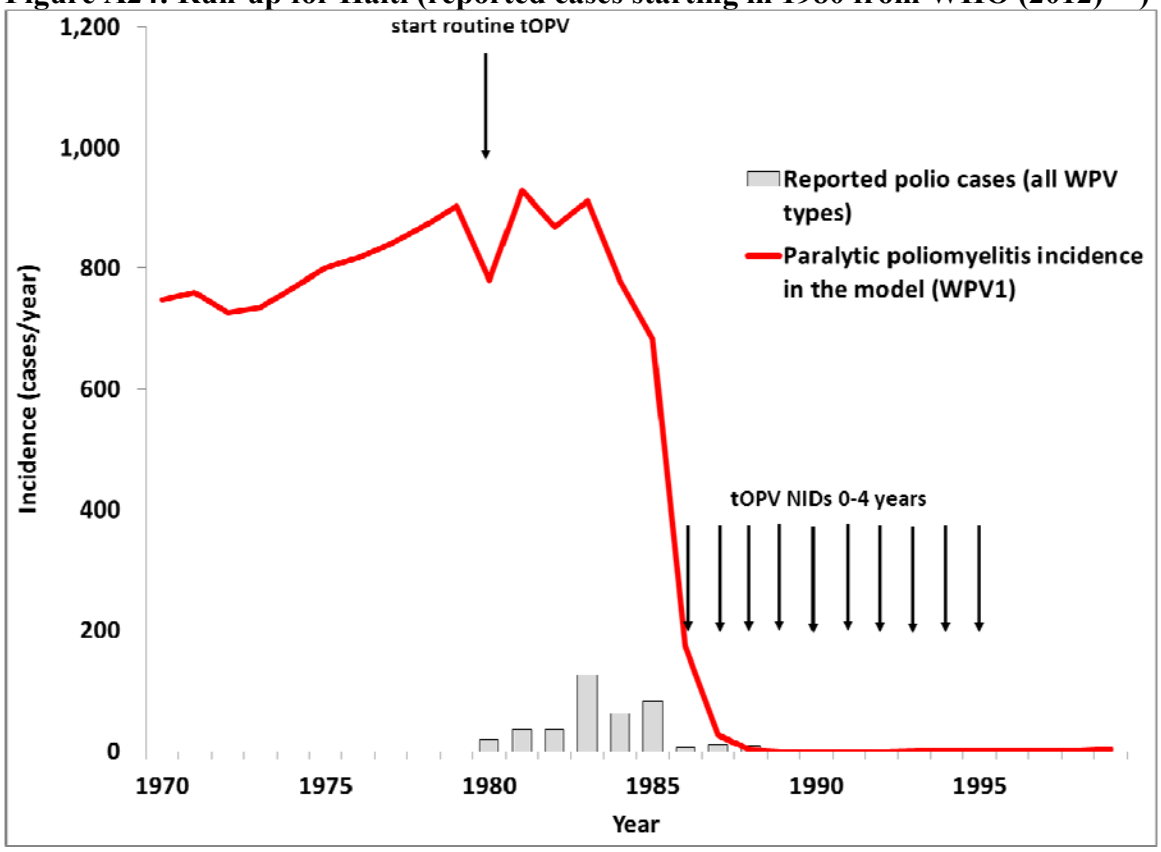

Figure A25: Run-up for Madura

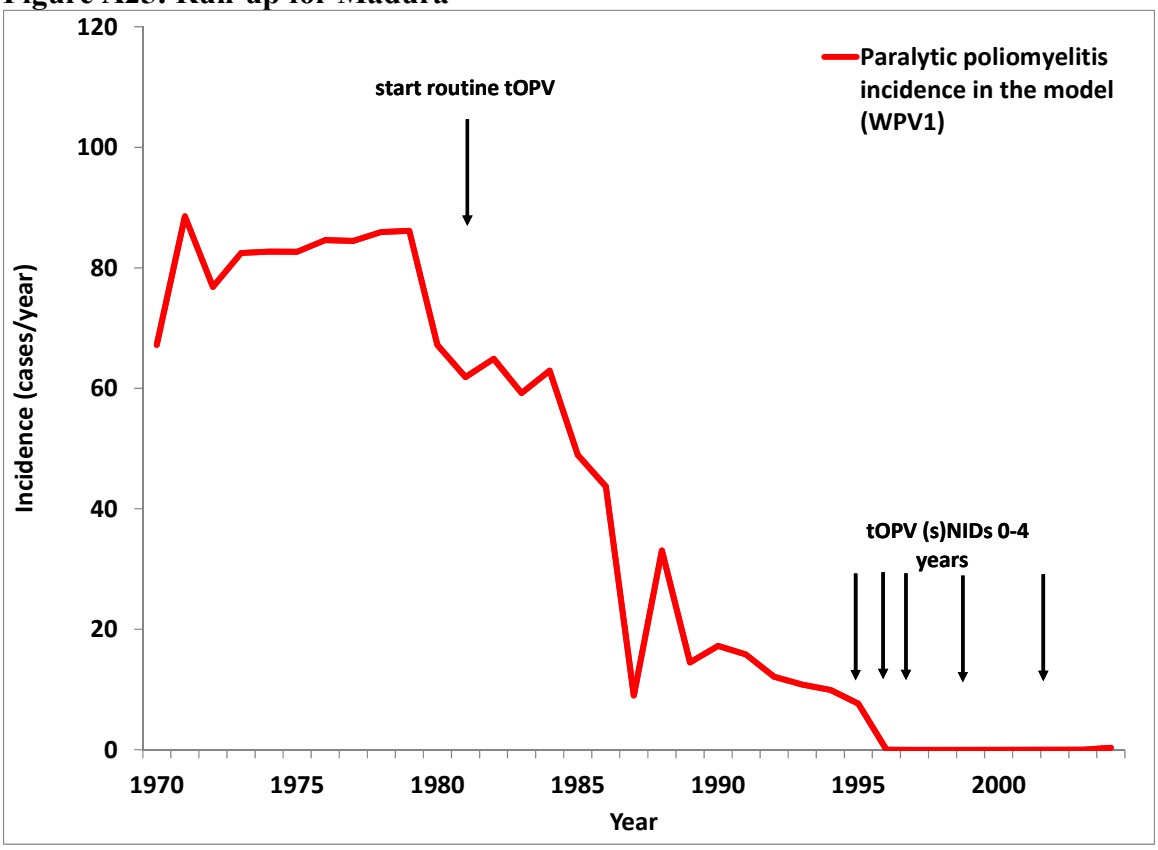

Figure A26: Run-up for Northern Nigeria (reported cases based on WHO data[24, 26])

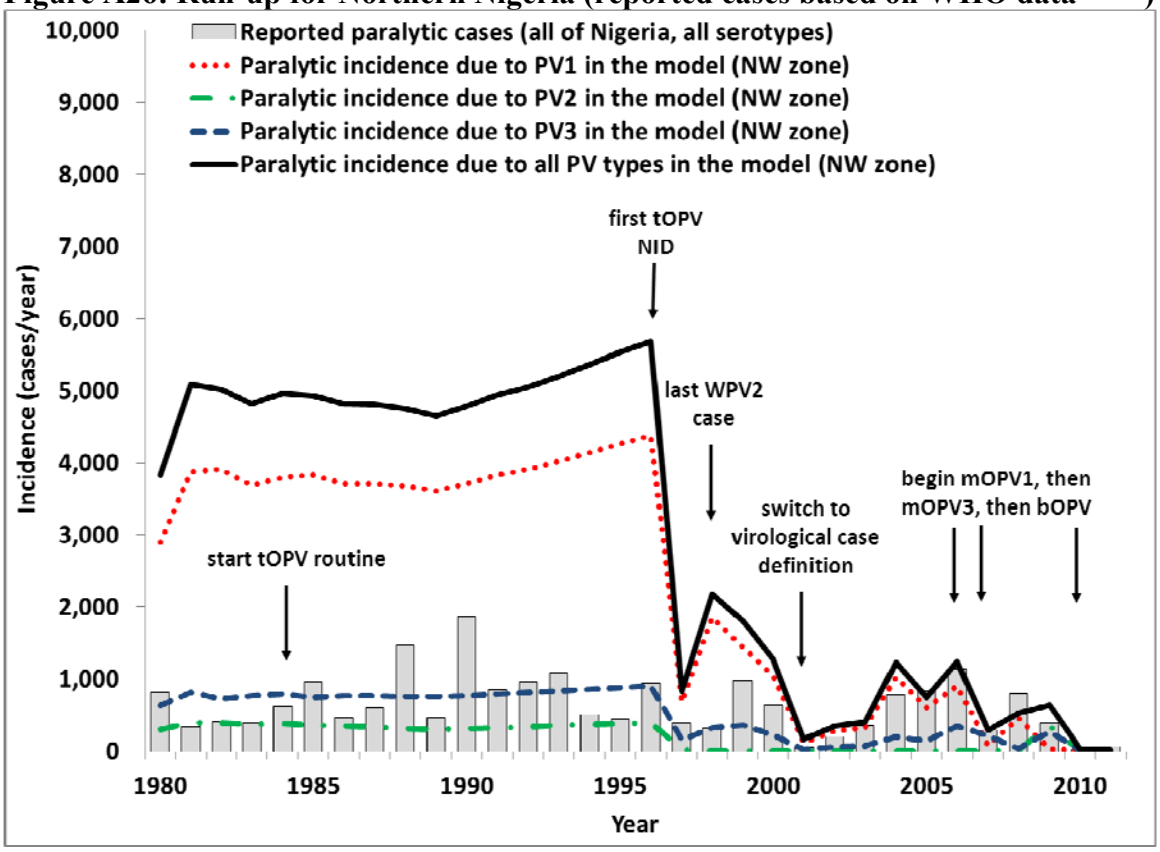

Figure A27: Run-up for northern India (reported cases based on WHO data[24, 26])

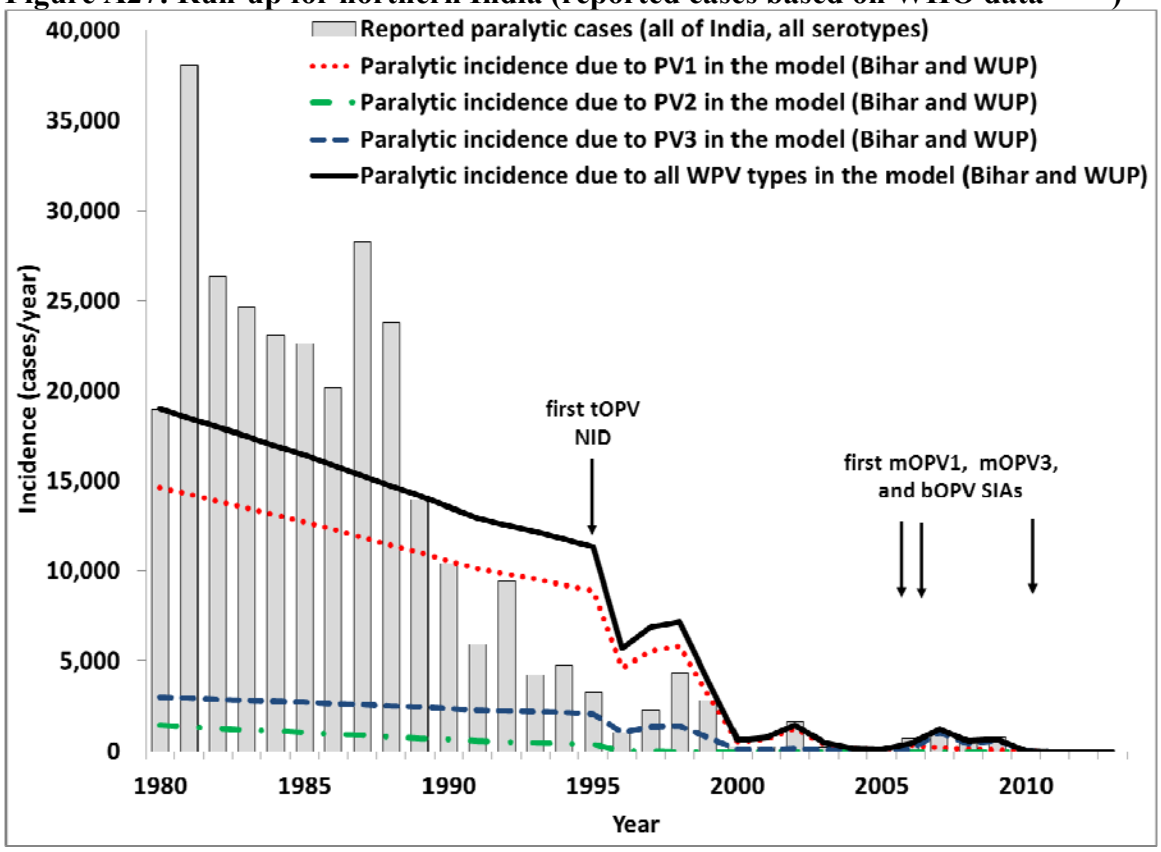

Table A1 shows the incidence of VAPP in the model (excluding The Netherlands, due to its minimal use of OPV, and Madura, where the total from 1997-2004 remains below 1 case due to the small population size), with comparisons to data provided in the notes when available. We typically observe increased non-recipient VAPP cases leading up to outbreaks (e.g., type 1 in Tajikistan in 2008 and 2009, or type 2 northern Nigeria in 2002-2004) given that relatively more susceptibles become infected secondarily versus from direct receipt of OPV, and that lower population immunity allows circulation of more reverted OPV-related viruses.

The results compare well with the reported US numbers due to direct calibration of the PIR for OPV and the shape parameter to these data. If we extrapolate the total of 4 cases during 1980-1995 for Albania to the entire country, then the resulting 8 VAPP cases approach the reported 11 cases during the same time period.[13] For Cuba, the model matches the total reported VAPP cases during 1963-1996. For India, we did not find data for Bihar and WUP specifically, but we found a report of VAPP in the entire country in 1999 that reported elevated numbers of type 1 non-recipient VAPP cases compared to developed countries and a similarly high contribution of type 3 to the total number of recipient VAPP cases[27] similar to our model. For Tajikistan, Haiti, and northern Nigeria, we did not find data on VAPP incidence.

Our model produces relatively high numbers of type 2 non-recipient VAPP cases in settings of very low OPV use (e.g., northern Nigeria and northern India before SIAs). This relates to the emergence of transmission in higher reversion stages for which we assume much higher PIRs (Figure A4), including a limited number (24 cases) due to FRPVs that emerge and die out during 1986-1997 in WUP in addition to the non-recipient VAPP cases shown in Table A1. The total annual incidence of VAPP per million surviving infants ranges from approximately 2.5 in the USA to almost 7 in Albania. Albania represents somewhat of an outlier because it reflects a population with relatively high routine immunization in the context of low pre-existing population immunity, which remains consistent with the observed high VAPP incidence in Albania.[13]

Table A1: Type-specific incidence of recipient and non-recipient VAPP in the model.

Situation and serotype	VAPP cases		
	Recipient	**Non-recipient**	**Total VAPP**
USA, 1980-1996[a]			
Type 1	2	6	8
Type 2	20	27	47
Type 3	46	26	72
Any type	57	101	158
Albania, 1980-1995[b]			
Type 1	< 1	2	2
Type 2	< 1	< 1	1
Type 3	< 1	2	2
Any type	< 1	4	4
Tajikistan, 1996-2009			
Type 1	< 1	3	4
Type 2	< 1	1	1
Type 3	1	2	3

Any type	1	6	8
Cuba, 1963-1996[c]			
Type 1	< 1	1	2
Type 2	3	2	5
Type 3	7	4	10
Any type	10	7	18
Haiti, 1990-1999			
Type 1	< 1	5	5
Type 2	1	2	3
Type 3	2	2	4
Any type	3	9	12
Northern Nigeria, 1984-2004			
Type 1	< 1	5	5
Type 2	4	43	47
Type 3	8	8	16
Any type	13	56	69
Northern India, 1980-2010[d]			
Type 1	1	39	40
Type 2	6	430	436
Type 3	19	45	64
Any type	26	538	564

Notes:

[a] See Table II for a comparison of these results with reported VAPP cases

[b] Diamanti et al. (1998)[13] reports 11 VAPP cases for the whole country during the same time period (the model incidence includes only half of the country), including 3 cases with onset of paralysis within 4-40 days of receipt of OPV, and the type distribution ambiguous due to isolation of multiple serotypes or isolation only from healthy contacts in a large fraction of VAPP cases

[c] Más Lago (1999)[8] reports a total of 18 VAPP cases during the same time period, including 12 with onset 11-28 days after receiving the first OPV dose, with PV2 isolated from 12 of 18 patients, type 3 from 5 patients, and both type 2 and 3 from 1 patient

[d] Kohler et al. (2002)[27] report 181 laboratory-confirmed VAPP cases for all of India during the year 1999, including 60 classified as recipient VAPP and 121 as non-recipient VAPP; 33%, 22%, and 33% of cases had only type 1, only type 2, and only type 3 isolated, respectively

Table A2 compares the force-of-infection to 0-4 year old fully susceptible individuals from all OPV-related viruses in the USA model to that reported among a small number of unvaccinated children by Chen et al. (1996),[28] as discussed in the main paper. Figure A28 shows the force-of-infection to 0-4 year olds from all OPV-related viruses after the second NID round in 1991, and the resulting cumulative proportion of fully susceptible infants infected as a function of the time born since the 2nd NID round. Table 14 lists the eventual cumulative percent infected at different time points. Given the absence of cases in Cuba and its role primarily as a situation that bounds the behavior of OPV reversion, we also demonstrate in Figure A29 that the force-of-infection in Cuba does not lead to cVDPVs over a range of potential R_0 assumptions for Cuba.

Table A2: Comparison of observations by Chen at al. (1996)[28] with model results for the USA

Quantity	Type 1	Type 2	Type 3
Proportion (95% CI) of unvaccinated children seropositive at 12-23 months, 1990-1991			
- Detroit (n=41)	0.17 (0.08-0.35)	0.34 (0.20-0.53)	0.10 (0.03-0.23)
- Houston (n=48)	0.07 (0.02-0.17)	0.24 (0.13-0.38)	0.15 (0.08-0.28)
Average annual force of infection of OPV-related virus required for observed proportion seropositive[c]			
- Detroit (n=41)	0.12 (0.06-0.29)	0.28 (0.15-0.50)	0.07 (0.02-0.17)
- Houston (n=48)	0.05 (0.01-0.12)	0.18 (0.09-0.32)	0.11 (0.06-0.22)
Average annual force of infection of OPV-related virus in the USA model, 1990-1991	0.17	0.24	0.08

Acronyms: CI=confidence intervals; OPV=oral poliovirus vaccine; USA=United States

Notes:

[a] Calculated as –ln(1-*proportion seropositive at 12-23 months*)/1.5

Figure A28: Secondary infections with all OPV-related viruses in Cuba

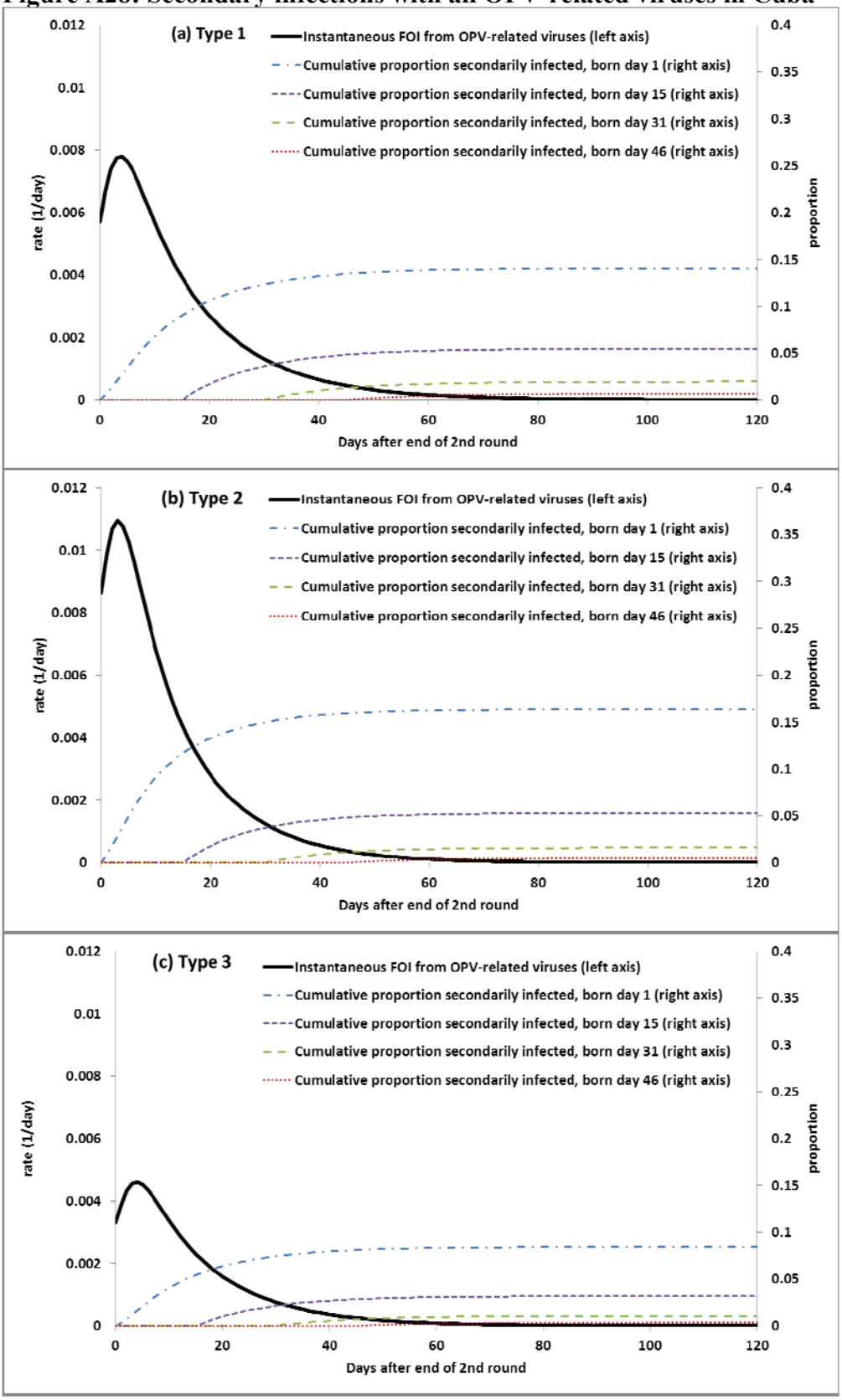

Figure A29: Force-of-infection (FOI) from all OPV-related viruses in Cuba, as a function about the assumed basic reproductive number (R_0).

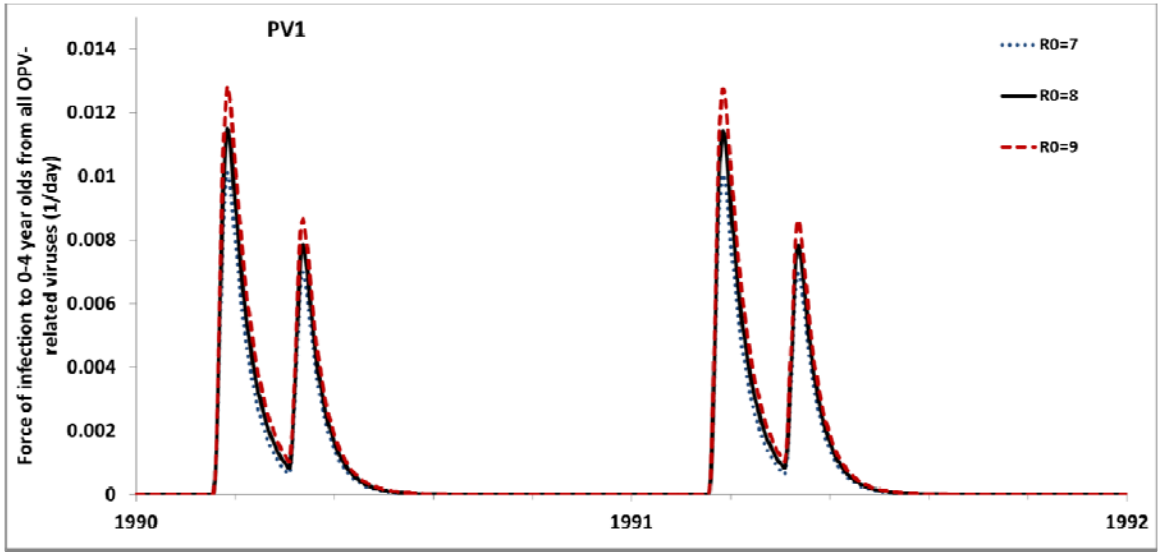

Reference:

1. Jacquez JA, Simon CP, Koopman J, Sattenspiel L, Perry T. Modeling and analyzing HIV transmission: The effect of contact patterns. Mathematical Biosciences 1988;92:119-199.
2. Lloyd AL. Realistic distributions of infectious periods in epidemic models: Changing patterns of persistence and dynamics. Theoretical Population Biology 2001;60(1):59-71.
3. Duintjer Tebbens RJ, Pallansch MA, Kew OM, Cáceres VM, Sutter RW, Thompson KM. A dynamic model of poliomyelitis outbreaks: Learning from the past to help inform the future. American Journal of Epidemiology 2005;162(4):358-372.
4. Duintjer Tebbens RJ, Pallansch MA, Chumakov KM, Halsey NA, Hovi T, Minor PD, Modlin JF, Patriarca PA, Sutter RW, Wright PF, Wassilak SGF, Cochi SL, Kim J-H, Thompson KM. Review and assessment of poliovirus immunity and transmission: Synthesis of knowledge gaps and identification of research needs. Risk Analysis: 2013.
5. Sterman J. Business dynamics: Systems thinking and modeling for a complex world. Boston, MA: McGraw-Hill; 2001.
6. Duintjer Tebbens RJ, Pallansch MA, Cochi SL, Wassilak SGF, Linkins J, Sutter RW, Aylward RB, Thompson KM. Economic analysis of the Global Polio Eradication Initiative. Vaccine 2011;29(2):334-343.
7. UN Population Division. World population prospects population database: The 2010 revision population database. 2012; Available at: http://esa.un.org/wpp/unpp/panel_indicators.htm, accessed April 2 2012.
8. Más Lago P. Eradication of poliomyelitis in Cuba: A historical perspective. Bulletin of the World Health Organization 1999;77(8):681-687.
9. Morris L, Witte JJ, Gardner P, Miller G, Henderson DA. Surveillance of poliomyelitis in the United States, 1962-65. Public Health Reports 1967;82(5):417-427.
10. Thompson KM, Duintjer Tebbens RJ. Retrospective cost-effectiveness analyses for polio vaccination in the United States. Risk Analysis 2006;26(6):1423-1440.
11. World Health Organization. WHO/UNICEF estimated coverage time series. WHO and UNICEF. 2012; Available at: http://www.who.int/entity/immunization_monitoring/data/coverage_estimates_series.xls, accessed April 4 2012.
12. Prevots DR, Ciofi degli Atti ML, Sallabanda A, Diamanti E, Aylward RB, Kakariqqi E, Fiore L, Ylli A, van der Avoort HG, Sutter RW, Tozzi AE, Panei P, Schinaia N, Genovese D, Oblapenko G, Greco D, Wassilak SG. Outbreak of paralytic poliomyelitis in Albania, 1996: High attack rate among adults and apparent interruption of transmission following nationwide mass vaccination. Clinical Infectious Diseases 1998;26(2):419-425.
13. Diamanti E, Ibrahimi B, Tafaj F, Mezini E, Dodbiba A, Dobi V, Catone S, Genovese D, Simeoni P, Fiore L. Surveillance of suspected poliomyelitis in Albania, 1980-1995: Suggestion of increased risk of vaccine associated poliomyelitis. Vaccine 1998;16(9):940-948.
14. State Committee on Statistics of the Repubic of Tajikistan. Tajikistan living standards measurement survey 2007. Dushanbe, Tajikistan: State Committee on Statistics of the Repubic of Tajikistan; 2009.
15. World Health Organization. Haiti. WHO and UNICEF estimates of immunization coverage: 2010 revision.2012; Available at: http://www.who.int/immunization_monitoring/data/hti.pdf, accessed April 17 2012.

16. Measure DHS. Demographic and health surveys, Haiti, 1994-95, 2000, and 2005-06. 2013; Available at: http://measuredhs.com/, accessed February 11 2013.
17. Kew O, Morris-Glasgow V, Landaverde M, Burns C, Shaw J, Garib Z, Andre J, Blackman E, Freeman CJ, Jorba J, Sutter R, Tambini G, Venczel L, Pedreira C, Laender F, Shimizu H, Yoneyama T, Miyamura T, van Der Avoort H, Oberste MS, Kilpatrick D, Cochi S, Pallansch M, de Quadros C. Outbreak of poliomyelitis in Hispaniola associated with circulating type 1 vaccine-derived poliovirus. Science 2002;296(5566):356-359.
18. Wringe A, Fine PE, Sutter RW, Kew OM. Estimating the extent of vaccine-derived poliovirus infection. PLoS One 2008;3(10):e3433.
19. Estívariz CF, Watkins M, Handoko D, Rusipah R, Deshpande J, Rana BJ, Irawan E, Widhiastuti D, Pallansch MA, Thapa A, Imari S. A large vaccine-derived poliovirus outbreak on Madura island--Indonesia, 2005. Journal of Infectious Diseases 2008;197(3):347-354.
20. Measure DHS. Demographic and health surveys, Nigeria 1990, 1999, 2003, and 2008.2012; Available at: http://measuredhs.com/, accessed August 20 2012.
21. Measure DHS. Demographic and health surveys, India, 1992-93, 1998-99, 2005-06. 2013; Available at: http://measuredhs.com/, accessed February 11 2013.
22. van den Hof S, Conyn-Van Spaendonck MA, de Melker HE, Geubbels E, Suijkerbuijk A, Talsma E, Plantinga A, Rümke H. The effects of vaccination, the incidence of target diseases. Bilthoven, The Netherlands: National Institute of Public Health and the Environment (RIVM); 1998. Report No.: 213676008.
23. Verlinde JD, Wilterdink JB. A small-scale trial on vaccination and revaccination with live attenuated polioviruses in the Netherlands. Presented at the First International Conference of Live Poliovirus Vaccine; Washington, D.C.: Pan American Sanitary Bureau; 1959; 355-366.
24. World Health Organization. Incidence series.2012; Available at: http://www.who.int/entity/immunization_monitoring/data/incidence_series.xls, accessed April 6 2012.
25. Rodriguez Cruz R. Cuba: Mass polio vaccination program, 1962-1982. Reviews of Infectious Diseases 1984;6(Suppl 2):S408-S412.
26. World Health Organization. Global Polio Eradication Initiative -- cases of wild poliovirus by country and by year 2000-2011. 2012; Available at: http://www.polioeradication.org/Dataandmonitoring/Poliothisweek/Wildpolioviruslist.aspx, accessed May 13 2012.
27. Kohler KA, Banerjee K, Gary Hlady W, Andrus JK, Sutter RW. Vaccine-associated paralytic poliomyelitis in India during 1999: Decreased risk despite massive use of oral polio vaccine. Bulletin of the World Health Organization 2002;80(3):210-216.
28. Chen RT, Hausinger S, Dajani AS, Hanfling M, Baughman AL, Pallansch MA, Patriarca PA. Seroprevalence of antibody against poliovirus in inner-city preschool children. Journal of the American Medical Association 1996;275(21):1639-1645.